Journal of Computational Physics 473 (2023) 111699

Contents lists available at ScienceDirect

Journal of Computational Physics

journal homepage: www.elsevier.com/locate/jcp

A dynamic mass transport method for Poisson-Nernst-Planck equations

Hailiang Liu [a,*], Wumaier Maimaitiyiming [b]

[a] Department of Mathematics, Iowa State University, USA
[b] Department of Mathematics, University of California Los Angeles, USA

ARTICLE INFO

Article history:
Received 20 May 2022
Received in revised form 14 September 2022
Accepted 16 September 2022
Available online 26 October 2022

Keywords:
PNP equations
Optimal transport
Wasserstein distance
Positivity
Energy dissipation

ABSTRACT

A dynamic mass-transport method is proposed for approximately solving the Poisson–Nernst–Planck (PNP) equations. The semi-discrete scheme based on the JKO type variational formulation naturally enforces solution positivity and the energy law as for the continuous PNP system. The fully discrete scheme is further formulated as a constrained minimization problem, shown to be solvable, and satisfy all three solution properties (mass conservation, positivity and energy dissipation) independent of time step size or the spatial mesh size. Numerical experiments are conducted to validate convergence of the computed solutions and verify the structure preserving property of the proposed scheme.

1. Introduction

In this paper, we consider a time-dependent system of Poisson-Nernst-Planck (PNP) equations. Such system has been widely used to describe charge transport in diverse applications such as biological membrane channels [10,13,47], electrochemical systems [2], and semiconductor devices [36,44].

PNP equations consist of Nernst–Planck (NP) equations that describe the drift and diffusion of ion species, and the Poisson equation that describes the electrostatic interaction. Such mean field approximation of diffusive ions admits several variants, and in non-dimensional form we consider the following

$$\partial_t \rho_i = \nabla \cdot [D_i(x)\,(\nabla \rho_i + z_i \rho_i \nabla \phi)], \quad x \in \Omega \subset \mathbb{R}^d, \quad t > 0, \tag{1.1a}$$

$$-\nabla \cdot (\epsilon(x) \nabla \phi) = f(x) + \sum_{i=1}^{s} z_i \rho_i, \tag{1.1b}$$

subject to initial data $\rho_i(x,0) = \rho_i^{in}(x) \geq 0$ $(i = 1, \cdots, s)$ and appropriate boundary conditions to be specified in section 2. The equations are valid in a bounded domain Ω with boundary $\partial\Omega$ and for time $t \geq 0$. Here $\rho_i = \rho_i(x,t)$ is the charge carrier density for the i-th species, and $\phi = \phi(x,t)$ the electrostatic potential. $D_i(x)$ is the diffusion coefficient, z_i is the rescaled charge. In the Poisson equation, $\epsilon(x)$ is the permittivity, $f(x)$ is the permanent (fixed) charge density of the system, s is the number of species.

* Corresponding author.
E-mail addresses: hliu@iastate.edu (H. Liu), wumaier@math.ucla.edu (W. Maimaitiyiming).

https://doi.org/10.1016/j.jcp.2022.111699
0021-9991/

Due to the wide variety of devices modeled by the PNP equations, computer simulation for this system of differential equations is of great interest. However, the PNP system is a strongly coupled system of nonlinear equations, also, the PNP system as a gradient flow can take very long time evolution to reach steady states. Hence, designing efficient and stable numerical methods for the PNP system remains an active area of research (see, e.g., [12,30,33,35,45,46]).

PNP system possesses two immediate properties: it preserves the non-negativity of ρ_i and conserves total mass. Therefore, we can consider non-negative initial data with mass one, so that the density is in the set of probability measures $\mathcal{P}(\Omega)$ on Ω. The third property is the dissipation of the total energy, which can be expressed as follows. Given energy

$$E = \int_\Omega \left(\sum_{i=1}^{s} \rho_i \log \rho_i + \frac{1}{2}(f + \sum_{i=1}^{s} z_i \rho_i)\phi \right) dx + B, \tag{1.2}$$

with boundary correction term B, the NP equation (1.1a) can be written as

$$\partial_t \rho_i = \nabla \cdot (\rho_i D_i(x) \nabla(\delta_{\rho_i} E)). \tag{1.3}$$

Differentiating the energy along solutions of the PNP system, one formally obtains the energy dissipation along the gradient flow

$$\frac{dE}{dt} = -\int_\Omega \sum_{i=1}^{s} D_i(x)\rho_i |\nabla(\log \rho_i + z_i \phi)|^2 dx \le 0,$$

which indicates that the solution evolves in the direction of steepest descent of the energy. This property entails a characterization of the set of stationary states, and provides a useful tool to study its stability. Numerical methods for (1.1) are desired to attain all three properties at the discrete level, which are rather challenging.

1.1. Related work

The most common numerical approach is the direct discretization of (1.1) using classical finite difference, finite volume, finite element, or discontinuous Galerkin methods [11,12,14–19,29–33,35,39,45,46]. Such methods are explicit or semi-implicit in time, so the per time computation is cheap. But it is often challenging to ensure both unconditional positivity and discrete energy decay simultaneously. The nonlinearity also complicates the way to obtain solutions when applying implicit or semi-implicit solvers.

Equation (1.3) with $s = 1$ and $D_i(x) = const$ reduces to the following scalar equation:

$$\partial_t \rho = \nabla \cdot (\rho \nabla(\delta_\rho E)). \tag{1.4}$$

It is now well understood since the pioneering works of Otto [23,41] that equations of the form of (1.4) can be interpreted as the gradient flow with respect to the quadratic Wasserstein metric $W_2(\cdot,\cdot)$. Such flow stems from an initial density and evolves following the steepest decreasing direction of a prescribed functional E. How to efficiently solve a gradient flow remains an intriguing question.

In contrast to the aforementioned direct PDE solvers, the minimizing movement scheme (see [1] and the references therein) respects the fact that the trajectory aims at optimizing the energy decay. With such a scheme, solutions of (1.4) are approximated by solving a sequence of minimization problems,

$$\rho^{n+1} = \text{argmin}_{\rho \in K} \left\{ \frac{1}{2\tau} W_2^2(\rho^n, \rho) + E(\rho) \right\}, \quad \rho^0 = \rho^{in}(x), \tag{1.5}$$

often called Jordan-Kinderlehrer-Otto (JKO) scheme after [23], which defines a sequence $\{\rho^n\}$ in the probability space K to approximate the solution $\rho(x, n\tau)$, where $\tau > 0$ is the time step. Since ρ^n is in the probability space, thus method (1.5) is positivity and mass preserving. The fact $W_2(\rho^n, \rho) \ge 0$ ensures the energy dissipation for any $\tau > 0$. In light of the favorable properties of the JKO scheme, there have been many works devoted to the computation of minimizers for problem (1.5). The main numerical difficulties arise in approximating the Wasserstein distance, and different approaches have been introduced to deal with this term; see, e.g., [7,8,24,25,38] for using the Lagrangian numerical methods to approximate the Wasserstein distance, and [4,6,9,27,28,37,42] for using the Eulerian numerical methods.

In our approach, we consider an Eulerian method based on Benamou-Brenier's dynamic formulation [3] and a second order spatial discretization. This reframes the problem as a convex optimization problem with linear PDE constraints. The base formulation we use extends the one in [26], with the goal here to obtain a faster numerical solver. The authors in [26] constructed the JKO type scheme for a two species PNP system with constant coefficient $D_i(x) = 1$ and $\epsilon(x) = 1$. The existence of the unique minimizer to the JKO scheme and convergence of the minimizer to the weak solution of the PNP system have been established in [26]. There are a few novel ingredients involved in our base variational formulation beyond that in [26]: (i) multi-species are considered, and the evolution of their density are strongly coupled; (ii) the diffusion-coefficient $D_i(x)$ for each species is varying in space, for which the underlying geodesic curve associated with the Wasserstein metric

is rather complex, instead of straight lines; and (iii) the general Poisson equation is dealt with as an additional linear constraint, instead of using the form of a compact expression in terms of the Newton potential [26]. To use either the classical JKO scheme for (1.4) or our formulation as a basis for numerical simulations of PNP systems, one must first develop a fully discrete approximation of the minimization problem at each step of the scheme. The fully discrete JKO-type scheme for the multi-species variable coefficient PNP system on a bounded domain has not been studied yet. This is what we aim to accomplish in this paper.

1.2. Contribution

In the general setting with mixed types of boundary conditions, we identify a unified form of the total energy functional which is dissipating along the solution trajectories (see sections 2.1–2.2). We also present (Theorem 2.2) lower energy bounds with coercivity for such a functional. These provide a solid basis for our approach.

Our main contributions are:

- We construct a Wasserstein-type distance and formulate a corresponding variational scheme. The update at each scheme step reduces to solving a constrained minimization problem, for which we prove unique solvability (Theorem 2.3). Three solution properties: mass conservation, positivity, and energy dissipation are shown to be preserved in time (Theorem 2.4). We should point out such beneficial properties from the W_2 based approach has already been recognized for a large class of gradient flows of form (1.4).
- We further convert the variational scheme into a dynamic formulation, which for variable diffusion coefficients extends the classical Bennamou-Breiner formulation. To reduce computational cost, we use a local approximation for the artificial time in the constraint transport equation by a one step difference and the integral in time by a one term quadrature. Such treatment was recently proposed in [28] for the aggregation equation to avoid the introduction on inner time stepping. Here we prove that the resulting minimization problem is a first order time consistent scheme for the PNP system (Theorem 2.5), as is expected.
- We present a fully discrete scheme – by coupling with a 2nd order finite difference method. The underlying principle for spatial discretization is to preserve the structure of Wasserstein metric in the discrete sense. We further prove the unique solvability (Theorem 3.1) of the fully-discrete scheme, exploiting the convexity property of the objective functional in a constraint fashion.
- We prove that for any fixed time step and spatial meth sizes, density positivity will be propagating over all time steps (Theorem 3.2). Such positivity-preserving property is proven by taking advantage of the presence of $\rho \log \rho$ in the energy functional. For general aggregation equations, this is not the case. Indeed, in work [28], Fisher information regularization is added to enforce solution positivity for an aggregation equation.
- The fully-discrete minimization problem reduces to a convex optimization problem with linear constraints, and can be solved by efficient optimization solvers. Our numerical tests are conducted with a simple projected gradient algorithm. Compared to the usual primal-dual-interior-penalty (PDIP) algorithm [40], our method is both robust and efficient– mainly because positivity is rigorously proven to hold without a restriction on time steps.
- Numerical results are provided to demonstrate the superior performance of the proposed method.

1.3. Organization

The paper is organized as follows. In the next section, we provide necessary background on the dynamical formulation of the PNP system, main solution properties and its relation with Wasserstein gradient flows. We then derive the semi-discrete scheme. In Section 3, we introduce a fully discrete scheme and study the properties of this scheme. Numerical algorithms are given in Section 4. Numerical results are provided in Section 5, and the paper is concluded in Section 6.

Notation. We use $[n]$ to denote $\{1, 2, \cdots, n\}$ for any natural number n. For vector ϕ (fully discrete case), its amplitude is denoted by $|\phi|$. For function ϕ, $\|\phi\|$ is its L^2 norm.

2. Model background and semi-discretization

In this section we briefly review the model setup and the corresponding Wasserstein gradient flow.

2.1. Boundary conditions

Boundary conditions are a critical component of the PNP model and determine important qualitative behaviors of the solution. Let Ω be a bounded domain with Lipschitz boundary $\partial\Omega$. We use the no-flux boundary condition for the NP equations, i.e.,

$$D_i(x)\left(\nabla\rho_i + z_i\rho_i\nabla\phi\right)\cdot\mathbf{n} = 0, \quad x \in \partial\Omega, \quad i = 1, \cdots, s. \tag{2.1}$$

Here, $\mathbf{n}$ is the outer unit normal at the boundary point $x \in \partial\Omega$.

The external electrostatic potential ϕ is influenced by applied potential, which can be modeled by prescribing a boundary condition. Here we consider a general form of boundary conditions:

$$\alpha\phi + \beta\epsilon(x)\frac{\partial\phi}{\partial\mathbf{n}} = \phi^b, \quad x \in \partial\Omega. \tag{2.2}$$

Here α, β are physical parameters such that $\alpha \cdot \beta \geq 0$, and $\phi^b = \phi^b(x,t)$ is a given function. With such setup, we are to solve the following initial-boundary value problem:

$$\begin{cases} \partial_t \rho_i = \nabla \cdot [D_i(x)(\nabla\rho_i + z_i\rho_i\nabla\phi)], & x \in \Omega, \quad t > 0, \ i = 1, \cdots, s, \\ -\nabla\cdot(\epsilon(x)\nabla\phi) = f(x) + \sum_{i=1}^s z_i\rho_i, & x \in \Omega, \quad t > 0, \\ \rho_i(x,0) = \rho_i^{in}(x) \geq 0, & x \in \Omega, \quad i = 1, \cdots, s, \\ (D_i(x)(\nabla\rho_i + z_i\rho_i\nabla\phi))\cdot\mathbf{n} = 0, & x \in \partial\Omega, \quad t > 0, \ i = 1, \cdots, s, \\ \alpha\phi + \beta\epsilon(x)\frac{\partial\phi}{\partial\mathbf{n}} = \phi^b, & x \in \partial\Omega, \quad t > 0. \end{cases} \tag{2.3}$$

Remark 2.1. (2.2) includes three typical forms: (i) the Robin boundary condition ($\alpha = 1, \beta > 0$) models a capacitor [14], (ii) the Dirichlet boundary condition ($\alpha = 1, \ \beta = 0$) models an applied voltage, and (iii) the Neumann boundary condition ($\alpha = 0, \ \beta = 1$) models surface changes. The case of pure Neumann boundary conditions requires the compatibility condition

$$\int_\Omega \left(f(x) + \sum_{i=1}^s z_i\rho_i^{in} \right) dx + \int_{\partial\Omega} \epsilon(x)\phi^b ds = 0, \tag{2.4}$$

and an additional constraint such as $\int_\Omega \phi(x,t)dx = 0$ so that ϕ is uniquely defined.

Any combination of these three types can be applied to ϕ on a disjoint partition of the boundary. In what follows, we set

$$\partial\Omega = \Gamma_D \cup \Gamma_N \cup \Gamma_R,$$

and on each part, one type of boundary condition is imposed, i.e.,

$$\alpha = \begin{cases} 1, & \text{on } \Gamma_D, \\ 0, & \text{on } \Gamma_N, \\ 1, & \text{on } \Gamma_R, \end{cases} \quad \beta = \begin{cases} 0, & \text{on } \Gamma_D, \\ 1, & \text{on } \Gamma_N, \\ \beta_R, & \text{on } \Gamma_R, \end{cases} \quad \phi^b = \begin{cases} \phi_D^b, & \text{on } \Gamma_D, \\ \phi_N^b, & \text{on } \Gamma_N, \\ \phi_R^b, & \text{on } \Gamma_R. \end{cases}$$

The existence and uniqueness of the solution for the nonlinear PNP boundary value problems with different boundary conditions have been studied in [22,34,43] for the 1D case and in [5,21] for multi-dimensions.

2.2. Energy functional: dissipation and coercivity

In the presence of homogeneous boundary conditions on ϕ, i.e., $\phi^b = 0$, the PNP system is energetically closed in the sense that the free energy functional associated to (1.1) is of form

$$E_0 = \int_\Omega \left(\sum_{i=1}^s \rho_i \log\rho_i + \frac{1}{2}(f + \sum_{i=1}^s z_i\rho_i)\phi \right) dx, \tag{2.5}$$

which along solution trajectories is dissipating in time. For general boundary conditions with $\phi^b \neq 0$, we need to modify the energy so that it is still dissipating along the solution of the PNP system. To this end, we differentiate (2.5) along the solution of (1.1), with integration by parts using (2.1), we have

$$\frac{d}{dt}E_0(\rho,\phi)(t) = -\int_\Omega \sum_{i=1}^s D_i(x)\rho_i|\nabla(\log\rho_i + z_i\phi)|^2 dx + \frac{1}{2}\int_{\partial\Omega} \epsilon(x)\left[\phi(\partial_n\phi)_t - (\partial_n\phi)\phi_t\right] ds.$$

Assume that ϕ^b does not depend on time, then $\alpha\phi_t + \beta\epsilon(x)\partial_n\phi_t = 0$ on $\partial\Omega$, this allows us to express the last term as

$$\frac{1}{2}\frac{d}{dt}\left[\int_{\Gamma_D} \epsilon(x)\phi_D^b\partial_n\phi ds - \int_{\Gamma_N} \phi_N^b\phi ds - \frac{1}{\beta_R}\int_{\Gamma_R} \phi_R^b\phi ds \right].$$

Thus the modified total energy functional can be taken as

$$E = E_0 - \frac{1}{2}\left[\int_{\Gamma_D} \epsilon(x)\phi_D^b \partial_n \phi ds - \int_{\Gamma_N} \phi_N^b \phi ds - \frac{1}{\beta_R}\int_{\Gamma_R} \phi_R^b \phi ds\right]. \tag{2.6}$$

Using the Poisson equation, the total energy can be rewritten as

$$E(\rho,\phi) = \int_\Omega \left(\sum_{i=1}^s \rho_i \log \rho_i + \frac{1}{2}\epsilon(x)|\nabla\phi|^2\right)dx - \int_{\Gamma_D} \epsilon(x)\phi_D^b \partial_n \phi ds + \frac{1}{2\beta_R}\int_{\Gamma_R} |\phi|^2 ds. \tag{2.7}$$

Proposition 2.1. *Assume that ϕ^b does not depend on time, then the extended energy functional (2.7) satisfies*

$$\frac{d}{dt}E(\rho,\phi)(t) = -\int_\Omega \sum_{i=1}^s D_i(x)\rho_i|\nabla(\log\rho_i + z_i\phi)|^2 dx \le 0, \quad t > 0, \tag{2.8}$$

along the solution of (1.1).

Recall that on Γ_D, the usual strategy for analysis is to transform it to the case with zero boundary value for ϕ. This way the modified energy would include an additional term called the external potential energy. For simplicity, we take $\phi_D^b = 0$, so that we have the following result.

Theorem 2.2. *(Lower bound and coercivity of E) Let Ω be an open, bounded Lipschitz domain, and ϕ^b be independent of time with $\phi_D^b = 0$, $\beta_R > 0$, and $\epsilon(x) \ge a > 0$. Then the energy of form*

$$E(\rho,\phi) = \int_\Omega \left(\sum_{i=1}^s \rho_i \log \rho_i + \frac{1}{2}\epsilon(x)|\nabla\phi|^2\right)dx + \frac{1}{2\beta_R}\int_{\Gamma_R} |\phi|^2 ds \tag{2.9}$$

is bounded from below. Moreover, there exist constants $c_0, c_1 > 0$ such that

$$E(\rho,\phi) \ge c_0\|\phi\|_{H^1}^2 - c_1. \tag{2.10}$$

Proof. For $\rho_i \ge 0$, we have $\int_\Omega \sum_{i=1}^s \rho_i \log(\rho_i) \ge -s|\Omega|/e =: -c_1$. For the ϕ-dependent part in E, we argue for all possible cases. For $\Gamma_D \ne \emptyset$ we have $\phi_D^b = 0$; for purely Neumann's condition we have the additional condition $\int_\Omega \phi(x)dx = 0$, in either case we can apply the Poincaré inequality or the Poincaré–Wirtinger inequality to conclude

$$\|\phi\|_{L^2}^2 \le c^*\|\nabla\phi\|_{L^2}^2$$

with constant c^* depending on the geometry of Ω, hence

$$E \ge -c_1 + \frac{a}{2}\|\nabla\phi\|_{L^2}^2 \ge c_0\|\phi\|_{H^1}^2 - c_1, \quad c_0 = \frac{a}{4}\min\{1, \frac{1}{c^*}\}.$$

For the case $\partial\Omega = \Gamma_R \cup \Gamma_N$ with $\Gamma_R \ne \emptyset$, we have

$$E(\rho,\phi) \ge \frac{1}{2}\min\{a, \beta_R^{-1}\}\tilde{E} - c_1$$

with $\tilde{E}(\phi) := \int_\Omega |\nabla\phi|^2 dx + \int_{\partial\Omega} |\phi|^2 ds$. We claim that

$$\tilde{E}(\phi) \ge c\|\phi\|_{H^1}^2 \quad \text{for some} \quad c > 0,$$

which can be proved with a contradiction argument. Since otherwise we can assume $\tilde{E}(\phi_n) < \frac{1}{n}\|\phi_n\|_{H^1}^2$. Set $w_n = \phi_n/\|\phi_n\|_{H^1}$, then $w_n \in H^1(\Omega)$ with

$$\|w_n\|_{H^1} = 1 \text{ and } \|\nabla w_n\|_{L^2}^2 < 1/n.$$

By the Rellich-Kondrachov theorem, we can extract a subsequence $\{w_{n_k}\}$ weakly converging to w in $H^1(\Omega)$ with $\nabla w_{n_k} \to 0$ weakly in $L^2(\Omega)$. This allows us to conclude $w \in H^1$, and $\nabla w = 0$. From $\int_{\Gamma_R} |w_{n_k}|^2 ds < 1/n_k$ and

$$\|w\|_{L^2(\Gamma_R)} \le \|w_{n_k}\|_{L^2(\Gamma_R)} + \|w_{n_k} - w\|_{L^2(\Gamma_R)} \le 1/\sqrt{n_k} + C\|w - w_{n_k}\|_{H^1},$$

we obtain $w = 0$ on Γ_R. Hence $w = 0$ a.e., this is a contradiction. We complete this case by taking $c_0 = \frac{c}{2}\min\{a, \beta_R^{-1}\}$. □

2.3. Wasserstein distance and JKO scheme for multi-density

In order to derive a variational scheme for the PNP system with multi-density, we need to introduce a Wasserstein-type distance. Motivated by the well-known characterization of the Wasserstein distance in a one-component fluid obtained by Benamou-Brenier [3], we consider to minimize a joint functional over the set

$$\begin{aligned} K := \{&\rho = (\rho_1, \cdots, \rho_s), u = (u_1, \cdots, u_s) : \\ &\partial_t \rho_i + \nabla \cdot (\rho_i u_i) = 0, \quad (\rho_i u_i) \cdot \mathbf{n} = 0 \quad \text{on } \partial\Omega \times [0,1], \\ &\rho_i \in \mathcal{P}(\Omega), \quad \rho_i(x,0) = \rho_i^0(x), \quad \rho_i(x,1) = \rho_i^1(x)\}. \end{aligned} \tag{2.11}$$

For the PNP system of two species $s = 2$ with $D_i(x) = 1$ and $\epsilon(x) = 1$ considered in [26], the distance inherited from the 2-Wasserstein distance is defined by

$$d^2(\rho^0, \rho^1) = \sum_{i=1}^{2} W_2^2(\rho_i^0, \rho_i^1).$$

This is equivalent to the minimization of the joint functional:

$$d^2(\rho^0, \rho^1) := \min_{(\rho,u)\in K} \sum_{i=1}^{2} \int_0^1 \int_\Omega |u_i|^2 \rho_i dx dt. \tag{2.12}$$

Here t is an artificial time and serves to characterize the optimal curve in the density space. Following [23], the authors in [26] constructed the following JKO scheme: Given a time step τ, the scheme defines a sequence ρ^n as

$$\rho^0 = \rho^{in}, \quad \rho^{n+1} = \arg\min_{\rho\in[\mathcal{P}(\Omega)]^2} \left\{ \frac{1}{2\tau} d^2(\rho^n, \rho) + \mathcal{E}(\rho) \right\}. \tag{2.13}$$

Here $\mathcal{E}$ is the total free energy, d^2 is the (squared) distance on the product space as defined in (2.12). One of the challenges in this program lies in handling the coupling terms, some intrinsic difficulties arise due to both the specific Poisson kernel and the system setting. Note that in [26] with $\epsilon(x) = 1$, the electrostatic potential ϕ in $E(\rho, \phi)$ is replaced by

$$\phi[\rho] = N * (f + \sum_{i=1}^{2} z_i \rho_i), \quad x \in \Omega,$$

so that $\mathcal{E}(\rho) = E(\rho, \phi[\rho])$. Here the kernel $N \sim C/|x|^{d-2}$ serves as a counterpart of the Green's function for the Newton potential in $\mathbb{R}^d$. Even with this treatment derivation of the corresponding Euler–Lagrange equations is quite delicate. We refer to [26] for further details.

In order to extend the above JKO-type scheme to the present setting, we face two new difficulties: (i) $D_i(x)$ is no longer a constant, the kinetic energy corresponding to the squared distance cost needs to be modified; (ii) $\epsilon(x)$ is a general non-negative function, ϕ cannot be expressed explicitly in terms of ρ. As for (i), we follow [20] and consider a modified functional

$$d^2(\rho^0, \rho^1) := \min_{(\rho,u)\in K} \sum_{i=1}^{s} \int_0^1 \int_\Omega D_i^{-1} |u_i|^2 \rho_i dx dt. \tag{2.14}$$

As for (ii), the Poisson equation is treated as a constraint in the resulting minimization problem. For ease of presentation we define

$$\mathcal{A} := \left\{ (\rho, \phi) : -\nabla \cdot (\epsilon(x) \nabla \phi) = f(x) + \sum_{i=1}^{s} z_i \rho_i, \quad \alpha\phi + \beta \frac{\partial \phi}{\partial \mathbf{n}} = \phi^b, x \in \partial\Omega, \rho \in [\mathcal{P}(\Omega)]^s \right\}. \tag{2.15}$$

For fixed $\rho^* \in [\mathcal{P}(\Omega)]^s$, and time step $\tau > 0$ we set

$$G_\tau(\rho, \phi) = \frac{1}{2\tau} d^2(\rho^*, \rho) + E(\rho, \phi), \quad (\rho, \phi) \in \mathcal{A}. \tag{2.16}$$

In order to define a discrete sequence of approximate solutions using the minimizing scheme, we present a result on the existence of minimizers of G_τ. To establish the uniqueness, we now prepare a technical lemma, with (iii) to be used later in the proof of Theorem 3.1.

Lemma 2.1. *Given X^0, X^1, let $X(\theta) = \theta X^0 + (1-\theta)X^1$ for any $\theta \in (0,1)$.*

(i) *If X^0, X^1 are vectors, then*

$$|X(\theta)|^2 - \theta|X^0|^2 - (1-\theta)|X^1|^2 = -\theta(1-\theta)|X^1 - X^0|^2. \tag{2.17}$$

(ii) *If $X^0 > 0, X^1 > 0$ are scalars, then*

$$X(\theta)\log X(\theta) - \theta X^0 \log X^0 - (1-\theta)X^1 \log X^1 = -\theta(1-\theta)(X^1 - X^0)^2 g(X^0, X^1; \theta), \tag{2.18}$$

for some positive function g depending on X^0, X^1 and θ.

(iii) *If $X^0 > 0, X^1 > 0, Y^0, Y^1$ are scalars, then*

$$\frac{(Y(\theta))^2}{X(\theta)} - \theta\frac{(Y^0)^2}{X^0} - (1-\theta)\frac{(Y^1)^2}{X^1} = -\theta(1-\theta)\frac{(X^1Y^0 - X^0Y^1)^2}{X^0X^1X(\theta)}. \tag{2.19}$$

Proof. We only prove (ii); as (i) and (iii) can be verified by a direct calculation. Note that

$$X(\theta)\log X(\theta) = \theta X^0 \log(X(\theta)) + (1-\theta)X^1 \log(X(\theta)). \tag{2.20}$$

Taylor's expansion of $\log(X(\theta)$ at X^0 and X^1, respectively, gives

$$\log(\theta X^0 + (1-\theta)X^1) = \log(X^0) + \frac{1}{X^0}(1-\theta)(X^0 - X^1) - \frac{(1-\theta)^2(X^1 - X^0)^2}{(\tilde{X}^0)^2},$$

where $\tilde{X}^0$ in between X^0 and $X(\theta)$, and

$$\log(\theta X^0 + (1-\theta)X^1) = \log(X^1) + \frac{1}{X^1} + \theta(X^1 - X^0) - \frac{\theta^2(X^1 - X^0)^2}{(\tilde{X}^1)^2},$$

where $\tilde{X}^1$ in between X^1 and $X(\theta)$. Substituting these into the right hand side of (2.20) leads to

$$\begin{aligned} X(\theta)\log X(\theta) =& \theta X^0 \log X^0 - \theta(1-\theta)^2\frac{X^0}{(\tilde{X}^0)^2}(X^1 - X^0)^2 \\ &+ (1-\theta)X^1 \log X^1 - \theta^2(1-\theta)\frac{X^1}{(\tilde{X}^1)^2}(X^1 - X^0)^2, \end{aligned}$$

this completes the proof of (ii) by defining $g(X^0, X^1, \theta) = \frac{(1-\theta)X^0}{(\tilde{X}^0)^2} + \frac{\theta X^1}{(\tilde{X}^1)^2} > 0$. □

Theorem 2.3. *(Existence of minimizers) Fix $\tau > 0$, and $\rho^* \in [\mathcal{P}(\Omega)]^s$. Then the functional $G_\tau(\rho, \phi)$ admits a unique minimizer on $\mathcal{A}$.*

Proof. By Theorem 2.2, G_τ is bounded from below on $\mathcal{A}$, hence there is a minimizing sequence (ρ^k, ϕ^k) and ρ^k is tight and uniformly integrable. By the Dunford–Pettis Theorem one may extract a subsequence such that $\rho^k \to \rho$ in $L^1(\Omega)$, which together with $\rho^k \in [\mathcal{P}(\Omega)]^s$ ensure that $\rho \in [\mathcal{P}(\Omega)]^s$. In addition, $E(\rho, \cdot)$ is also coercive in ϕ because of (2.10), i.e.,

$$E(\rho, \phi) \geq c_0\|\phi\|_1^2 - c_1.$$

Hence one may extract a subsequence such that $\phi^k \to \phi$ weakly in $H^1(\Omega)$. The weak L^1 lower semi-continuity (l.s.c.) of the squared Wasserstein distance can be easily adapted to the present case. The lower semicontinuity of E with respect to weak convergence can be seen from the following inequality

$$E(\rho^k, \phi^k) \geq E(\rho, \phi) + \int_\Omega \left[\sum_{i=1}^s \ln\rho_i(\rho_i^k - \rho_i) + \epsilon(x)\nabla\phi \cdot (\nabla\phi^k - \nabla\phi)\right] dx + \frac{\alpha}{\beta}\int_{\partial\Omega} \phi(\phi^k - \phi) ds.$$

Putting all these together we claim that the limit is a minimizer.

Finally, the uniqueness comes from the fact that the admissible set $\mathcal{A}$ is convex w.r.t. linear interpolation and that the total free energy is jointly strictly convex in (ρ, ϕ) on $\mathcal{A}$. More precisely, we argue as follows. Let $\theta \in (0,1)$, then $\rho(\theta) = \theta\rho^0 + (1-\theta)\rho^1$ is a convex linear combination for ρ^0 and ρ^1. Let ϕ^0 and ϕ^1 be obtained from the Possion equation, corresponding to ρ^0 and ρ^1, respectively. Then $\phi(\theta) = \theta\phi^0 + (1-\theta)\phi^1$ must be the solution to the Poisson equation corresponding to $\rho(\theta)$. For the energy of form (2.9), we evaluate $E(\rho(\theta), \phi(\theta))$ term by term to determine whether it is strictly convex. Using (2.18) for $\rho_i^l = X^l$ and (2.17) for $X^l = \nabla\phi^l$ in Ω, and (2.17) for $X^l = \phi^l$ on Γ_R, respectively, we obtain

$$E(\rho(\theta),\phi(\theta)) - \theta E(\rho^0,\phi^0) - (1-\theta)E(\rho^1,\phi^1) = -\theta(1-\theta)I$$

with

$$I = \int_\Omega \left(\sum_{i=1}^{s} (\rho_i^1 - \rho_i^0)^2 g(\rho_i^0, \rho_i^1; \theta) + \frac{1}{2}\epsilon(x)|\nabla(\phi^1 - \phi^0)|^2 \right) dx + \frac{1}{2\beta_R}\int_{\Gamma_R} (\phi^1 - \phi^0)^2 ds.$$

Convexity of E follows from $I \geq 0$. Actually this inequality is strict, unless $\rho^0 = \rho^1, \phi^0 = \phi^1$, which can be derived from letting $I = 0$. Hence $E(\rho,\phi)$ is strictly convex under two linear constraints. □

We are now ready to present a variational scheme formulation – a JKO-type scheme for (2.3): given time step $\tau > 0$, recursively we define a sequence $\{\rho^n, \phi^n\}$ by

$$\rho^0 = \rho^{\text{in}}, \quad (\rho^{n+1}, \phi^{n+1}) = \arg\min_{(\rho,\phi)\in\mathcal{A}} \left\{ \frac{1}{2\tau} d^2(\rho^n, \rho) + E(\rho,\phi) \right\}. \tag{2.21}$$

Theorem 2.4. *(Solution properties of scheme (2.21))*

(i) *(Probability-preserving) If $\rho^n \in [\mathcal{P}(\Omega)]^s$, so is ρ^{n+1};*
(ii) *(Unconditionally energy stability) the inequality*

$$E(\rho^{n+1},\phi^{n+1}) + \frac{1}{2\tau} d^2(\rho^n, \rho^{n+1}) \leq E(\rho^n,\phi^n)$$

holds for any $n \geq 0$. Furthermore,

$$\sum_{n=0}^{\infty} d^2(\rho^n, \rho^{n+1}) \leq 2\tau (E(\rho^0,\phi^0) - \inf_{(\rho,\phi)\in\mathcal{A}} E(\rho,\phi)). \tag{2.22}$$

Proof. (i) The constraint $\mathcal{A}$ ensures that $\rho^n \in [\mathcal{P}(\Omega)]^s$ which is inherited from initial data; namely the method is both positivity and mass preserving.

(ii) From the definition of the minimizer, it follows

$$E(\rho^{n+1},\phi^{n+1}) + \frac{1}{2\tau} d^2(\rho^n, \rho^{n+1}) \leq E(\rho^n,\phi^n).$$

Here we used $d^2(\rho,\rho) = 0$ for any $\rho \in [\mathcal{P}(\Omega)]^s$. Finally, summation over n yields (2.22). □

These properties in Theorem 2.4 are highly desirable for PNP systems, yet quite difficult to achieve by other methods without a restriction on time steps. But these properties are quite natural for W_2 based approach, and easy to verify as long as the involved optimization step is well-posed.

2.4. Semi-discrete JKO scheme

We proceed to obtain a computable formulation. Let $m_i = \rho_i u_i$, the dynamic formulation of the distance $d^2(\cdot,\cdot)$ in (2.21) can be expressed as: given $\rho^n(x)$, we have

$$(\rho^{n+1},\phi^{n+1}) = \arg\min_{(\rho,\phi)\in\mathcal{A},m} \left\{ \frac{1}{2\tau} \sum_{i=1}^{s} \int_0^1 \int_\Omega F(\rho_i, m_i) D_i^{-1} dx dt + E(\rho(\cdot,1), \phi(\cdot,1)) \right\}, \tag{2.23}$$
$$\text{s.t.} \quad \partial_t \rho_i + \nabla\cdot(m_i) = 0, \quad m_i \cdot \mathbf{n} = 0, \quad x \in \partial\Omega, \ \rho(x,0) = \rho^n.$$

Here t is an artificial time, and

$$F(\rho_i, m_i) = \begin{cases} \frac{|m_i|^2}{\rho_i} & \text{if } \rho_i > 0, \\ 0 & \text{if } (\rho_i, m_i) = (0,0), \\ +\infty & \text{otherwise.} \end{cases}$$

The use of m_i has enhanced the functional convexity in m_i and made the transport constraint linear (see Breiner [3]), yet causing difficulties for solutions near $\rho_i = 0$. We shall prove for the fully discrete case that positivity of ρ_i^n is preserved for all n. Another computational overhead with (2.23) is dealing with the artificial time $t \in [0,1]$ which is induced by the

optimal transport flow. To overcome this issue, we follow [28] with a local approximation in the artificial time: approximate the derivative in t in the constraint transport equation by a one step difference and the integral in time in the objective function by a one term quadrature. We thus obtain the following scheme:

$$\begin{aligned}(\rho^{n+1},\phi^{n+1}) = \arg\min_{(\rho,\phi)\in\mathcal{A},m}&\left\{\frac{1}{2\tau}\sum_{i=1}^{s}\int_{\Omega}F(\rho_i,m_i)D_i^{-1}dx+E(\rho,\phi)\right\},\\ \text{s.t.}\quad &\rho_i-\rho_i^n+\nabla\cdot(m_i)=0,\quad m_i\cdot\mathbf{n}=0,\quad x\in\partial\Omega.\end{aligned}\tag{2.24}$$

Theorem 2.5. *The positive minimizer of the variational problem (2.24) is a first-order time consistent scheme for the PNP system.*

Proof. Let (2.24) admit a minimizer with $\rho>0$. We can derive optimal conditions by the Lagrange multiplier method. Define the Lagrangian as

$$\begin{aligned}L(\rho,\phi,m,v,\xi) :=&\frac{1}{2\tau}\sum_{i=1}^{s}\int_{\Omega}F(\rho_i,m_i)D_i^{-1}dx+E(\rho,\phi)+\int_{\partial\Omega}\xi(\alpha\phi+\beta\partial_n\phi-\phi^b)ds\\ &+\sum_{i=1}^{s}\int_{\Omega}v_i(\rho_i-\rho_i^n+\nabla\cdot m_i)dx+\int_{\Omega}v_{s+1}(f+\sum_{i=1}^{s}z_i\rho_i+\nabla\cdot(\epsilon(x)\nabla\phi))dx.\end{aligned}$$

The optimality conditions for $x\in\Omega$ are

$$\begin{aligned}&\frac{\delta L}{\delta\rho_i}=0 \quad \text{implies} \quad -\frac{1}{2\tau}\frac{||m_i||^2}{\rho_i^2}D_i^{-1}+\log(\rho_i)+1+\frac{1}{2}z_i\phi+v_i+z_iv_{s+1}=0,\quad i=1,\cdots,s,\\ &\frac{\delta L}{\delta\phi}=0 \quad \text{implies} \quad \frac{1}{2}(f+\sum_{i=1}^{s}z_i\rho_i)+\nabla\cdot(\epsilon(x)\nabla v_{s+1})=0,\\ &\frac{\delta L}{\delta m_i}=0 \quad \text{implies} \quad \frac{1}{\tau}\frac{m_i}{\rho_i}D_i^{-1}-\nabla\cdot v_i=0,\quad i=1,\cdots,s,\\ &\frac{\delta L}{\delta v_i}=0 \quad \text{implies} \quad \rho_i-\rho_i^n+\nabla\cdot m_i=0,\quad i=1,\cdots,s,\\ &\frac{\delta L}{\delta v_{s+1}}=0 \quad \text{implies} \quad f+\sum_{i=1}^{s}z_i\rho_i+\nabla\cdot(\epsilon(x)\nabla\phi)=0.\end{aligned}$$

For $x\in\Omega$, we thus have

$$v_i=\frac{1}{2\tau}\frac{||m_i||^2}{\rho_i^2}D_i^{-1}-\log(\rho_i)-1-\frac{1}{2}z_i\phi-z_iv_{s+1},\quad m_i=\tau D_i\rho_i\nabla v_i$$

and

$$\nabla\cdot(\epsilon(x)\nabla v_{s+1})=\frac{1}{2}\nabla\cdot(\epsilon(x)\nabla\phi).$$

On $\partial\Omega$, from integrating by parts in calculating δL there remain the following boundary terms

$$\int_{\partial\Omega}\epsilon(x)\delta(\partial_n\phi)v_{s+1}ds-\int_{\partial\Omega}\epsilon(x)\delta\phi\partial_nv_{s+1}ds+\int_{\partial\Omega}v_i\delta m_i\cdot\mathbf{n}ds,$$

where the last term vanishes due to the constraint $m_i\cdot\mathbf{n}=0$. In addition, we need also consider terms arising from

$$\delta B+\delta\int_{\partial\Omega}\xi(\alpha\phi+\beta\partial_n\phi-\phi^b)ds.$$

Upon careful regrouping, we have two cases to distinguish:

(i) for $\beta\neq0$, the correction term B in the energy (1.2) is given by

$$B=\frac{1}{2\beta}\int_{\partial\Omega}\phi^b\phi ds.$$

We obtain

$$\epsilon(x)v_{s+1} + \beta\epsilon(x)\xi = 0, \quad -\epsilon(x)\partial_n v_{s+1} + \alpha\xi + \frac{1}{2\beta}\phi^b = 0, \quad \text{on } \partial\Omega;$$

(ii) For $\beta = 0$.

The correction term B in the energy (1.2) is given by

$$B = -\frac{1}{2\alpha}\int_{\partial\Omega} \epsilon(x)\phi^b \partial_n \phi ds,$$

from which we have

$$\epsilon(x)v_{s+1} - \frac{1}{2\alpha}\epsilon(x)\phi^b + \beta\xi = 0, \quad -\epsilon(x)\partial_n v_{s+1} + \alpha\xi = 0, \quad \text{on } \partial\Omega.$$

These ensure that we always have

$$\alpha v_{s+1} + \beta\partial_n v_{s+1} = \frac{1}{2}\phi^b \quad \text{on } \partial\Omega.$$

Take $\psi = \frac{1}{2}\phi - v_{s+1}$ we have

$$\nabla\cdot(\epsilon(x)\nabla\psi) = 0, x \in \Omega; \alpha\psi + \beta\partial_n\psi = 0 \text{ on } \partial\Omega.$$

By the uniqueness of the Poisson problem we conclude $\psi \equiv 0$ or $\psi = \text{cost}$ if $\alpha = 0$, i.e.,

$$v_{s+1} \equiv \frac{1}{2}\phi + cost.$$

Combining the above we have the following update

$$\rho_i = \rho_i^n + \tau\nabla\cdot(D_i\rho_i\nabla(\log(\rho_i) + z_i\phi)) + O(\tau^2).$$

This says scheme (2.24) is a first order time discretization of the PNP system (2.3). □

Remark 2.2. A natural question arises: is the discrete transport still preserves positivity of ρ_i. We shall address this issue for the fully discrete scheme, for which positivity propagation is rigorously established in Theorem 3.2.

3. Numerical method

In this section, we detail the spatial discretization. The underlying principle for spatial discretization is to preserve the structure of Wasserstein metric tensor in the discrete sense.

3.1. Spatial discretization

We only consider the discretization in one dimensional setting. Let $\Omega = [a,\ b]$ be the computational domain partitioned into N cells $I_j = [x_{j-\frac{1}{2}},\ \ x_{j+\frac{1}{2}}]$, with mesh size $h = (b-a)/N$ and cell center at $x_j = x_{j-\frac{1}{2}} + \frac{1}{2}h,\ j \in \{1, 2, \cdots, N\}$. Let numerical solution be $\{\phi_j\}_{j=1}^N$, $\{\rho_{ij}\}_{j=1}^N$, and $\{m_{i,j+1/2}\}_{j=1}^{N-1}$ on two grids x_j and $x_{j+1/2}$, respectively. We define the difference operator by

$$(D_h v)_{j+1/2} := \frac{v_{j+1} - v_j}{h}, \quad (d_h v)_j := \frac{v_{j+1/2} - v_{j-1/2}}{h}$$

and average operator by

$$\hat{v}_j := \frac{v_{j+1/2} + v_{j-1/2}}{2}.$$

We also use $\epsilon_{j+1/2} = \epsilon(x_{j+1/2})$, $f_j = f(x_j)$, and $D_{ij} = D_i(x_j)$.

The transport constraint is discretized with central difference in space as follows:

$$\rho_{ij} - \rho_{ij}^n + d_h(m_i)_j = 0, \tag{3.1}$$

and the zero boundary conditions $m_{i,1/2} = m_{i,N+1/2} = 0$ are applied.

For the Possion equation, we consider the Robin boundary condition at both ends, other types of boundary conditions can be handled in same fashion. We introduce two ghost values ϕ_0 and ϕ_{N+1} for conveniently approximating the boundary condition (2.2) with center differences:

$$\frac{\phi_0+\phi_1}{2}-\beta_a\epsilon(a)\frac{\phi_1-\phi_0}{h}=\phi^b(a),\quad \frac{\phi_{N+1}+\phi_N}{2}+\beta_b\epsilon(b)\frac{\phi_{N+1}-\phi_N}{h}=\phi^b(b). \tag{3.2}$$

This together with the center difference approximation of the Poisson equation gives a coupled linear system:

$$\begin{aligned}&(h+2\beta_a\epsilon(a))\phi_0+(h-2\beta_a\epsilon(a))\phi_1-2h\phi^b(a)=0,\\ &-d_h(\epsilon D_h\phi)_j-f_j-\sum_{i=1}^{s}z_i\rho_{ij}=0,\quad j=1,\cdots,N,\\ &(h-2\beta_b\epsilon(b))\phi_N+(h+2\beta_b\epsilon(b))\phi_{N+1}-2h\phi^b(b)=0.\end{aligned} \tag{3.3}$$

We denote such linear constraint by $L_h(\phi,\rho)=0$. The objective function then writes as

$$\begin{aligned}\mathcal{F}_h(\rho,m,\phi)=&\frac{h}{2\tau}\sum_{j=1}^{N}\sum_{i=1}^{s}\frac{\hat{m}_{i,j}^2}{\rho_{i,j}}D_{i,j}^{-1}+h\sum_{j=1}^{N}\left(\sum_{i=1}^{s}\rho_{i,j}\log\rho_{i,j}+\frac{\epsilon_j}{8h^2}(\phi_{j+1}-\phi_{j-1})^2\right)\\ &+\frac{1}{8\beta_a}(\phi_0+\phi_1)^2+\frac{1}{8\beta_b}(\phi_N+\phi_{N+1})^2,\end{aligned} \tag{3.4}$$

which is a second order spatial approximation of the objective functional in (2.24).

To formulate an admissible set for the discrete minimization problem, let the discrete probability distribution set be: for $\delta>0$

$$P_{h,\delta}=\left\{(\rho_1,\cdots,\rho_N):\quad \rho_j\geq\delta,\quad h\sum_{j=1}^{N}\rho_j=1\right\}.$$

Then the constraint set for (ρ,ϕ) becomes

$$\mathcal{A}_{h,\delta}=\{(\rho,\phi):\quad \rho\in[P_{h,\delta}]^s,\quad L_h(\phi,\rho)=0\}.$$

Thus the admissible set for all (ρ,m,ϕ) collectively can be written as

$$V_{h,\delta}^n=\{(\rho,m,\phi):\quad \rho_{ij}-\rho_{ij}^n+d_h(m_i)_j=0,\quad (\rho,\phi)\in\mathcal{A}_{h,\delta}\}$$

with $m_{i,1/2}=m_{i,N+1/2}=0$. Thus we have

$$V_{h,\delta}^n\subset\mathbb{R}^{s(2N-1)+N+2}.$$

The one time update with the fully discrete scheme is to find

$$\rho^{n+1}=\arg\min_{u\in V_{h,\delta}^n}\left\{\mathcal{F}_h(u)\right\},\quad u:=(\rho,m,\phi). \tag{3.5}$$

Theorem 3.1. *(Unique solvability) Fix $\tau>0, h>0$ and $\{\rho_i^n\in P_{h,\delta}\}_{i=1}^s$ for some $\delta>0$. Then the function $\mathcal{F}_h(\rho,m,\phi)$ admits a unique minimizer in $V_{h,\delta}^n\subset\mathbb{R}^{s(2N-1)+N+2}$.*

Proof. The proof proceeds in two steps:

Step 1 (Admissible set is non-empty and convex) The conservative form of the transport constraint ensures that we always have

$$h\sum_{j=1}^{N}\rho_{ij}=1\quad i\in[s].$$

For fixed $\delta>0$, take $\rho_{ij}\geq\delta$, we can uniquely determine m by

$$m_{i,j+1/2}=\frac{1}{h}\sum_{l=1}^{j}(\rho_{il}-\rho_{il}^n), \tag{3.6}$$

for $j = 1, \cdots, N-1$. From the linear system $L(\phi, \rho) = 0$ we obtain a unique $\phi = (\phi_0, \cdots, \phi_{N+1})$ in terms of f_j and $\rho_{ij} \geq \delta$, since its coefficient matrix is tridiagonal, and diagonally dominated. Hence the admissible set $V^n_{h,\delta}$ is non-empty. The fact that both the transport constraint and $L(\phi, \rho) = 0$ are linear implies that the set $V^n_{h,\delta}$ is convex in $\mathbb{R}^{s(2N-1)+N+2}$.

Step 2 (Objective function is strictly convex under constraints) With $u = (\rho, m, \phi)$, for any $u^0, u^1 \in V_{h,\delta}$ and $\theta \in (0,1)$, $u(\theta) = \theta u^0 + (1-\theta)u^1$ is a convex linear combination of u^0 and u^1. In addition, as argued in the proof of Theorem 2.3, we have $u(\theta) \in V_{h,\delta}$. We now show the convexity of $\mathcal{F}_h(u)$ by directly calculating

$$\mathcal{F}_h(u(\theta)) - \theta\mathcal{F}_h(u^0)) - (1-\theta)\mathcal{F}_h(u^1) = -\theta(1-\theta)(I_1 + I_2 + I_3),$$

where applying Lemma 2.1 to each term I_i, we have

$$\begin{aligned}
I_1 =& \frac{h}{2\tau}\sum_{i=1}^{s}\sum_{j=1}^{N}\frac{(\rho^1_{i,j}\hat{m}^0_{i,j} - \rho^0_{i,j}\hat{m}^1_{i,j})^2}{\rho^0_{i,j}\rho^1_{i,j}\rho(\theta)_{i,j}} \geq 0, \quad \text{by } (iii) \text{ of Lemma 2.1}\\
I_2 =& h\sum_{i=1}^{s}\sum_{j=1}^{N} g_{i,j}(\rho^0_{i,j}, \rho^1_{i,j}, \theta)(\rho^0_{i,j} - \rho^1_{i,j})^2 \geq 0, \ \text{ by } (ii) \text{ of Lemma 2.1}\\
I_3 =& \frac{1}{8h}\sum_{j=1}^{N}\epsilon_j[(\phi^0_{j+1} - \phi^0_{j-1}) - (\phi^1_{j+1} - \phi^1_{j-1})]^2 \quad \text{by } (i) \text{ of Lemma 2.1}\\
&+ \frac{1}{8\beta_a}[(\phi^0_0 + \phi^0_1) - (\phi^1_0 + \phi^1_1)]^2 + \frac{1}{8\beta_b}[(\phi^0_N + \phi^0_{N+1}) - (\phi^1_N + \phi^1_{N+1})]^2 \geq 0.
\end{aligned}$$

Convexity of $\mathcal{F}_h$ follows from $I_1 + I_2 + I_3 \geq 0$. To establish strictly convexity we only need to show $I_1 + I_2 + I_3 = 0$ must lead to $u^0 = u^1$. We argue as follows.

Clearly the equality holds only when $I_1 = I_2 = I_3 = 0$. From $I_2 = 0$ it follows $\rho^0 = \rho^1$. This when combined with $I_1 = 0$ implies $\hat{m}^0_{i,j} = \hat{m}^1_{i,j}$, which together with $m^l_{i,1/2} = m^l_{i,N+1/2} = 0$ yields $m^0 = m^1$. Finally we show $\phi^0 = \phi^1$ must also hold. Set $\xi_j = \phi^0_j - \phi^1_j$ for $j = 0, \cdots, N+1$, then $I_3 = 0$ corresponds to the system of linear equations $\xi_0 + \xi_1 = 0$, $\xi_N + \xi_{N+1} = 0$ and $\xi_{j+1} - \xi_{j-1} = 0$, for $j = 1, \cdots, N$. This obviously admits non-zero solutions. From the constraint for ϕ near the boundary we have

$$\phi^0_0 + \phi^0_1 = 2\phi^b(a) + \frac{\beta_a}{h}\epsilon(a)(\phi^0_1 - \phi^0_0), \quad \phi^1_0 + \phi^1_1 = 2\phi^b(a) + \frac{\beta_a}{h}\epsilon(a)(\phi^1_1 - \phi^1_0),$$

this implies $\xi_0 + \xi_1 = \frac{\beta_a}{h}\epsilon(a)(\xi_1 - \xi_0)$. Using also $\xi_0 + \xi_1 = 0$, we can conclude $\xi_0 = \cdots = \xi_{N+1} = 0$, therefore $\phi^0 = \phi^1$. Hence $\mathcal{F}_h(u)$ is strictly convex on $V_{h,\delta}$. □

The last issue is to find a threshold for δ so to ensure that solution positivity for the PNP system is propagated at all time steps.

Theorem 3.2. *(Positivity propagation) There exists $\delta_0 > 0$ such that the minimizer does not touch the boundary of $V^n_{h,\delta}$ for all $0 < \delta \leq \delta_0$. This implies that $\rho^n > 0$ for all $n > 0$ as long as $\rho^0 > 0$.*

Proof. We use a contradiction argument: suppose there exists a minimizer u^* to the optimization problem (3.5) touching the boundary of $V^n_{h,\delta}$ at some grid points $j_1 < \cdots < j_k$ with $1 \leq k \leq N-1$ for ρ_i, that is

$$\rho^*_{i,j_1} = \cdots = \rho^*_{i,j_k} = \delta.$$

From $h\sum_{j=1}^{N}\rho^*_{i,j} = 1$, we see that $\delta < \frac{1}{b-a}$. Since $\mathcal{F}_h$ is convex and differentiable, we only need to find $u \in \mathcal{A}_{h,\delta}$ such that

$$\nabla\mathcal{F}_h(u^*)\cdot(u - u^*) < 0. \tag{3.7}$$

Note that both m and ϕ can be uniquely determined by ρ from the constraints, it suffices to first choose ρ and then express all components of u in terms of ρ. Let $\rho^*_{i,j_{k+1}}$ be the maximum component in vector ρ^*_i, using $h\sum_{j=1}^{N}\rho^*_{i,j} = 1$ we thus have

$$\frac{1}{b-a} < \rho^*_{i,j_{k+1}} < \frac{1}{h} = \frac{N}{b-a}. \tag{3.8}$$

Without loss of generality, we assume $j_{k+1} > j_k$, and

$$\rho^*_{i,j} \geq \delta + r_p(h), \quad j_p < j < j_{p+1}, \quad p = 1, \cdots, k, \tag{3.9}$$

where $r_p(0)=0$ and $r_p(h)>0$ for $h>0$ small. This can be justified by approximation for sufficiently small h. Fix $h>0$, we take for $0<\gamma<\frac{1}{k}(\frac{1}{b-a}-\delta)$,

$$\rho_{l,j}=\begin{cases}\delta+\gamma, & l=i,\ j=j_1,\cdots,j_k,\\ \rho^*_{i,j_{k+1}}-\gamma k, & l=i,\ j=j_{k+1},\\ \rho^*_{l,j}, & \text{else.}\end{cases}$$

Hence $\tilde{u}=u-u^*$ can be determined by

$$\tilde{\rho}_{l,j}=\rho_{l,j}-\rho^*_{lj}=\begin{cases}\gamma, & l=i,\ j=j_1,\cdots,j_k,\\ -\gamma k, & l=i,\ j=j_{k+1},\\ 0, & \text{else.}\end{cases}$$

Using $\tilde{m}=m-m^*$ and formula (3.6) for both m and m^*, we have

$$\tilde{m}_{l,j+1/2}=\frac{1}{h}\sum_{p=1}^{j}\tilde{\rho}_{l,p}=\begin{cases}\frac{1}{h}b_j\gamma, & l=i,\ j_1\le j\le j_{k+1}-1,\\ 0, & \text{else,}\end{cases}\tag{3.10}$$

for $0\le b_j\le k$. Hence

$$0\le\hat{\tilde{m}}_{i,j}\le\frac{k\gamma}{h},\quad j_1\le j\le j_{k+1}.$$

For $\tilde{\phi}=\phi-\phi^*$, using (3.3) for both ϕ and ϕ^*, we obtain $A\tilde{\phi}=[0,z_ih^2\tilde{\rho}_i,0]^\top$, where the coefficient matrix A is non-singular, more precisely, $\tilde{\phi}$ solves

$$\begin{aligned}&(h+2\beta_a\epsilon(a))\tilde{\phi}_0+(h-2\beta_a\epsilon(a))\tilde{\phi}_1=0,\\ &-\epsilon_{j-1/2}\tilde{\phi}_{j-1}+2\hat{\epsilon}_j\tilde{\phi}_j-\epsilon_{j+1/2}\tilde{\phi}_{j+1}=h^2z_i\tilde{\rho}_{i,j}\quad j=1,\cdots,N,\\ &(h-2\beta_b\epsilon(b))\tilde{\phi}_N+(h+2\beta_b\epsilon(b))\tilde{\phi}_{N+1}=0.\end{aligned}$$

The solution of this linear system can be expressed as

$$\tilde{\phi}_l=\gamma h^2(c_l-kd_l)z_i,\quad l=0,1,\cdots,N+1$$

for some c_l,d_l depending on the coefficients in the above system. The above preparation yields

$$\begin{aligned}&\nabla\mathcal{F}_h(u^*)\cdot(u-u^*)=\nabla\mathcal{F}_h(u^*)\cdot\tilde{u}\\ &=\sum_{l=1}^{s}\sum_{j=1}^{N}\partial_{\rho_{l,j}}\mathcal{F}_h(u^*)\tilde{\rho}_{l,j}+\sum_{l=1}^{s}\sum_{j=1}^{N-1}\partial_{m_{l,j+1/2}}\mathcal{F}_h(u^*)\tilde{m}_{l,j+1/2}+\sum_{j=0}^{N+1}\partial_{\phi_j}\mathcal{F}_h(u^*)\tilde{\phi}_j\\ &=\gamma\left[\sum_{p=1}^{k}\partial_{\rho_{i,j_p}}\mathcal{F}_h(u^*)-k\partial_{\rho_{i,j_{k+1}}}\mathcal{F}_h(u^*)\right]+\sum_{j=j_1}^{j_{k+1}-1}\partial_{m_{i,j+1/2}}\mathcal{F}_h(u^*)\tilde{m}_{i,j+1/2}+\sum_{j=0}^{N+1}\partial_{\phi_j}\mathcal{F}_h(u^*)\tilde{\phi}_j\\ &=:I_1+I_2+I_3.\end{aligned}$$

In order to estimate I_1,I_2,I_3 we also need to bound u^* in terms of ρ^*. From (3.6) and (3.8) we have

$$|m^*_{i,j+1/2}|\le\frac{1}{h}\sum_{l=1}^{j}\rho^*_{il}\le\frac{Nj}{(b-a)h}\Rightarrow|\hat{m}^*_{i,j}|\le\frac{N^2}{(b-a)h}=Nh^{-2}.$$

For ϕ^* satisfying $A\phi^*=h[2\phi^b(a),h(f+\sum_{i=1}^{s}z_i\rho^*_i),2\phi^b(b)]^\top$, we have

$$|\phi^*|\le h|A^{-1}|[2\phi^b(a),h(f+\sum_{i=1}^{s}z_i\rho^*_i),2\phi^b(b)]^\top|=:C^*_\phi.$$

We proceed as follows: from the definition of the objective function

$$\begin{aligned}\mathcal{F}_h(u)=&\frac{h}{2\tau}\sum_{j=1}^{N}\sum_{i=1}^{s}\frac{\hat{m}^2_{i,j}}{\rho_{i,j}}D^{-1}_{i,j}+h\sum_{j=1}^{N}\left(\sum_{i=1}^{s}\rho_{i,j}\log\rho_{i,j}+\frac{\epsilon_j}{8h^2}(\phi_{j+1}-\phi_{j-1})^2\right)\\ &+\frac{1}{8\beta_a}(\phi_0+\phi_1)^2+\frac{1}{8\beta_b}(\phi_N+\phi_{N+1})^2,\end{aligned}$$

given in (3.4) we have

$$
\begin{aligned}
I_1 &= \gamma \sum_{p=1}^{k}\left[-\frac{h}{2\tau}\cdot\frac{(\hat{m}^*_{i,j_p})^2}{(\rho^*_{i,j_p})^2}D^{-1}_{i,j_p}+h(1+\log\rho^*_{i,j_p})\right]-\gamma k\left[-\frac{h}{2\tau}\cdot\frac{(\hat{m}^*_{i,j_{k+1}})^2}{(\rho^*_{i,j_{k+1}})^2}D^{-1}_{i,j_{k+1}}+h(1+\log\rho^*_{i,j_{k+1}})\right]\\
&= -\frac{\gamma h}{2\tau\delta^2}\sum_{p=1}^{k}(\hat{m}^*_{i,j_p})^2D^{-1}_{i,j_p}+\gamma hk\log\delta+\frac{\gamma kh}{2\tau}\frac{(\hat{m}^*_{i,j_{k+1}})^2}{(\rho^*_{i,j_{k+1}})^2}D^{-1}_{i,j_{k+1}}-\gamma hk\log\rho^*_{i,j_{k+1}}\\
&\le -\frac{\gamma h}{2\tau\delta^2}\sum_{p=1}^{k}(\hat{m}^*_{i,j_p})^2D^{-1}_{i,j_p}+\gamma hk\log\delta+\frac{\gamma kN^4}{2\tau h}D^{-1}_{i,j_{k+1}}+\gamma hk\log(b-a)\\
&= -\frac{\gamma h}{2\tau\delta^2}\sum_{p=1}^{k}(\hat{m}^*_{i,j_p})^2D^{-1}_{i,j_p}+\frac{\gamma kN^4}{2\tau h}D^{-1}_{i,j_{k+1}}+\gamma hk\log\delta(b-a).
\end{aligned}
$$

Next, we estimate I_2:

$$
\begin{aligned}
I_2 &= \frac{h}{2\tau}\sum_{j=j_1}^{j_{k+1}-1}\left(\frac{\hat{m}^*_{i,j}}{\rho^*_{i,j}}D^{-1}_{i,j}+\frac{\hat{m}^*_{i,j+1}}{\rho^*_{i,j+1}}D^{-1}_{i,j+1}\right)\tilde{m}_{i,j+1/2}\\
&= \frac{h}{\tau}\sum_{j=j_1}^{j_{k+1}-1}\frac{\hat{m}^*_{i,j}}{\rho^*_{i,j}}D^{-1}_{i,j}\hat{\tilde{m}}_{i,j}+\frac{h}{2\tau}\left(-\frac{\hat{m}^*_{i,j_1}}{\rho^*_{i,j_1}}D^{-1}_{i,j_1}\tilde{m}_{i,j_1-1/2}+\frac{\hat{m}^*_{i,j_{k+1}}}{\rho^*_{i,j_{k+1}}}D^{-1}_{i,j_{k+1}}\tilde{m}_{i,j_{k+1}-1/2}\right)\\
&= \frac{h}{\tau}\sum_{p=1}^{k}\frac{\hat{m}^*_{i,j_p}}{\delta}D^{-1}_{i,j_p}\hat{\tilde{m}}_{i,j_p}+\frac{h}{\tau}\sum_{p=1}^{k}\sum_{j=j_p+1}^{j_{p+1}-1}\frac{\hat{m}^*_{i,j}}{\rho^*_{i,j}}D^{-1}_{i,j}\hat{\tilde{m}}_{i,j}+\frac{h}{2\tau}\cdot\frac{\hat{m}^*_{i,j_{k+1}}}{\rho^*_{i,j_{k+1}}}D^{-1}_{i,j_{k+1}}\tilde{m}_{i,j_{k+1}-1/2}\\
&\le \frac{h}{\tau}\cdot\frac{k\gamma}{h}\left(\sum_{p=1}^{k}\frac{|\hat{m}^*_{i,j_p}|}{\delta}D^{-1}_{i,j_p}+\sum_{p=1}^{k}\sum_{j=j_p+1}^{j_{p+1}-1}D^{-1}_{i,j}\frac{Nh^{-2}}{\delta+r_p(h)}+\frac{N^2}{h}D^{-1}_{i,j_{k+1}}\right)\\
&\le \frac{k\gamma}{\tau}\left(\frac{\eta}{2\delta^2}\sum_{p=1}^{k}(\hat{m}^*_{i,j_p})^2D^{-1}_{i,j_p}+\frac{1}{2\eta}\sum_{p=1}^{k}D^{-1}_{i,j_p}+\frac{N}{h^2}\sum_{p=1}^{k}\sum_{j=j_p+1}^{j_{p+1}-1}\frac{D^{-1}_{i,j}}{r_p(h)}+\frac{N^2}{h}D^{-1}_{i,j_{k+1}}\right),\quad\forall\eta>0.
\end{aligned}
$$

Take η so that $k\eta=h$, we have

$$
I_2\le\frac{\gamma h}{2\tau\delta^2}\sum_{p=1}^{k}(\hat{m}^*_{i,j_p})^2D^{-1}_{i,j_p}+C_1,\quad C_1:=\frac{k^2\gamma}{2\tau h}\sum_{p=1}^{k}D^{-1}_{i,j_p}+\frac{Nk\gamma}{\tau h^2}\sum_{p=1}^{k}\sum_{j=j_p+1}^{j_{p+1}-1}\frac{D^{-1}_{i,j}}{r_p(h)}+\frac{N^2k\gamma}{\tau h}D^{-1}_{i,j_{k+1}}.
$$

Note that

$$
\partial_{\phi_j}\mathcal{F}_h(u^*)=\frac{1}{4h}\left[\epsilon_{j-1}(\phi^*_j-\phi^*_{j-2})+\epsilon_{j+1}(\phi^*_j-\phi^*_{j+2})\right]\quad j=2,\cdots,N-1,
$$

this together with derivatives involving boundary terms allows us to estimate I_3:

$$
\begin{aligned}
I_3 &\le |\partial_\phi\mathcal{F}_h(u^*)|\cdot|\tilde{\phi}|\\
&\le \frac{1}{h}(|\epsilon|+\beta_a^{-1}+\beta_b^{-1})C^*_\phi\cdot\gamma|z|(|c|+k|d|)h^2=C_0C^*_\phi h.
\end{aligned}
$$

For $\delta<\frac{1}{2(b-a)}$, we can take $\gamma k=\frac{1}{2(b-a)}$ such that $k\gamma<1/(b-a)-\delta$ still holds. Hence

$$
\begin{aligned}
I_1+I_2+I_3 &\le \gamma hk\log\delta(b-a)+\frac{\gamma kN^4}{2\tau h}D^{-1}_{i,j_{k+1}}+C_1+C_0C^*_\phi h\\
&= \frac{1}{2N}\log\delta(b-a)+\frac{N^3}{4\tau h^2}D^{-1}_{i,j_{k+1}}+C_1+C_0C^*_\phi h<0
\end{aligned}
$$

provided $\delta<\delta_0$ with

$$
\delta_0:=\frac{1}{b-a}\min\left\{\exp\left(-\frac{N^4}{2\tau h^2}D^{-1}_{i,j_{k+1}}-2NC_1-2C_0C^*_\phi Nh\right),\frac{1}{2}\right\}.
$$

This gives (3.7) as we intended to show. Such contradiction allows us to conclude that a minimizer at nth step can only occur in the interior of V^n_{h,δ_0} for some $\delta_0 > 0$. In order to show such solution positivity can propagate, we start from $\rho^0 > 0$. Based on the above conclusion we recursively have

$$\rho^{n+1} \in V^n_{h,\delta} \subset V^n_{h,\delta_0}.$$

This completes the proof. □

4. Optimization algorithms

In this section, we discuss numerical techniques for solving the constrained optimization problem (3.5). Let $u = (\rho, m, \phi)$, (3.5) can be written as

$$\min_u \mathcal{F}_h(u), s.t. \quad Au = b, \quad Su \geq \delta, \tag{4.1}$$

where $\mathcal{F}_h(u)$ is defined in (3.4), $Au = b$ is the linear system corresponding to the constraints (3.1) and (3.3), and S is the selection matrix that only selects ρ component in u.

A simple method to solve (4.1) is the following update:

$$\tilde{u}^{n+1} = u^n - \eta G \nabla_u \mathcal{F}_h(u^n),$$

with the projection matrix defined by

$$G = I - A^\top (AA^\top)^{-1} A,$$

which ensures $A\tilde{u}^{n+1} = b$ if $Au^n = b$. One then applies another projection

$$u^{n+1} = \Pi(\tilde{u}^{n+1}),$$

so that $\rho^{n+1}_{ij} \geq \delta$.

Algorithm 1: PG Algorithm.

Input: $A, b, u^n, K = Iter_{max}$, and ϵ.
Output: u^{n+1}
initialization;
$G = I - A^T(AA^T)^{-1}A, \quad u^{(0)} = u^n$.
for $k = 1 : K$ **do**
- Compute the update direction by

$$v = -G\nabla_u \mathcal{F}_h(u^{(k-1)})$$

- Use backtracking to determine step size η;
- Update to get

$$\tilde{u} = u^{(k-1)} + \eta v$$

- Projection $u^{(k)} = \Pi(\tilde{u})$;

if $||Au^{(k)} - b|| + ||\eta v|| \leq \epsilon$ **then**
  Stop the iteration;
end
end
$u^{n+1} = u^{(k)}$.

The positivity propagation property stated in Theorem 3.2 ensures that $Su \geq \delta$ will be fulfilled by the scheme as long as $\rho^0 \geq \delta$ for δ suitably small. Hence in our numerical tests the second projection Π is not enforced, where we select

$$\delta = \max\{\min\{h^2, \tau\}, \min\{\rho^{in}_i(x_j)\}\} > 0.$$

In summary, the numerical solutions $\rho^n_{i,j}$ and ϕ^n_j are updated with the following algorithm:

Table 1
Accuracy for Example 5.1 with $\tau = h$.

h	ρ_1 error	order	ρ_2 error	order	ϕ error	order
1/10	2.67958E-02	-	9.80117E-03	-	1.17890E-03	-
1/20	1.27689E-02	1.06937	4.12484E-03	1.24862	5.46161E-04	1.11004
1/40	6.20098E-03	1.04207	1.91422E-03	1.10758	3.18396E-04	0.77850
1/80	3.04165E-03	1.02764	9.21957E-04	1.05399	1.74525E-04	0.86739

Algorithm 2: Algorithm for the fully discrete scheme.

Input: $\rho_i^{in}(x)$, final time T, and discretization parameters h, τ, $\delta > 0$
Output: $\rho_{i,j}^n$, ϕ_j^n for $n = 1, \cdots, T/\tau$.
initialization: $u^0 = (\rho^0, m^0, \phi^0)$ with
$\rho_{ij}^0 = \max\{\rho_i^{in}(x_j), \delta\}$.
$m_{i,j}^0 = 0$, and ϕ_j^0 is obtained by solving (3.2) with $\rho_{i,j}^0$.
for $n = 1 : T/\tau$ **do**
  $\rho^{n+1} = \arg\min_{u \in V_{h,\delta}^n} \left\{ \mathcal{F}_h(u) \right\}$ with Algorithm 1.
end

Remark 4.1. One may also apply other optimization solvers such as the Primal-Dual Interior-Point algorithm (PDIP) [40, Chapter 19]) to solve the minimization problem in Algorithm 2, as long as a positive lower bound for densities can be properly enforced.

5. Numerical tests

In this section, we present a selected set of numerical tests to demonstrate the convergence and properties of the proposed scheme. In all tests, the tolerance for PG method is set as 10^{-6}.

Errors are measured in the following discrete l_2 norm:

$$err = \left(\sum_{1 \le j \le N} h |u_j^n - U_j^n|^2 \right)^{1/2}.$$

Here u_j^n and U_j^n denotes the numerical solutions and reference solutions at (x_j, t_n). In what follows we take $u_j^n = \rho_{i,j}^n$, or ϕ_j^n at time $t = n\tau$.

5.1. 1D multiple species

We apply our scheme to solve the 1D two-species PNP system (1.1) and verify the proven properties.

Example 5.1 *(Accuracy test).* We consider the following PNP system

$$\begin{aligned} \partial_t \rho_1 &= \partial_x \left(\partial_x \rho_1 + \rho_1 \partial_x \phi \right), \\ \partial_t \rho_2 &= \partial_x \left(\partial_x \rho_2 - \rho_2 \partial_x \phi \right), \\ -\partial_x^2 \phi &= \rho_1 - \rho_2, \end{aligned} \tag{5.1}$$

in $[-1,\ 1]$ and $t > 0$. This is (1.1) with $D_1 = D_2 = \epsilon = 1$, $q_1 = 1$, $q_2 = -1$, and $f(x) = 0$. The initial and boundary conditions are chosen as

$$\begin{aligned} &\rho_1^{in}(x) = 2 - x^2, \quad \rho_2^{in}(x) = 2 + sin(\pi x), \\ &\phi(0,t) = -1,\ \phi(1,t) = 1. \end{aligned} \tag{5.2}$$

In the accuracy test, we consider the numerical solutions obtained by $h = 1/320$ and $\tau = 1/10000$ as the reference solution. Our scheme is unconditionally energy stable, hence no CFL condition on the time step is needed. Formally the scheme is first order accurate in time, and second order accurate in space. Accuracy test is done in the following manner: we set the time step as $\tau = h$ to confirm the first order accuracy in time, and set $\tau = h^2$ to confirm the second order accuracy in space. The errors and orders at $t = 0.5$ are listed in Table 1 and Table 2, respectively.

Table 2
Accuracy for Example 5.1 with $\tau = h^2$.

h	ρ_1 error	order	ρ_2 error	order	ϕ error	order
1/10	9.00817E-03	-	3.13854E-03	-	1.42932E-03	-
1/20	2.22285E-03	2.01882	7.47122E-04	2.07068	3.62387E-04	1.97973
1/40	5.36781E-04	2.05001	1.78121E-04	2.06849	9.15204E-05	1.98537
1/80	1.15944E-04	2.21091	3.79348E-05	2.23126	2.35563E-05	1.95798

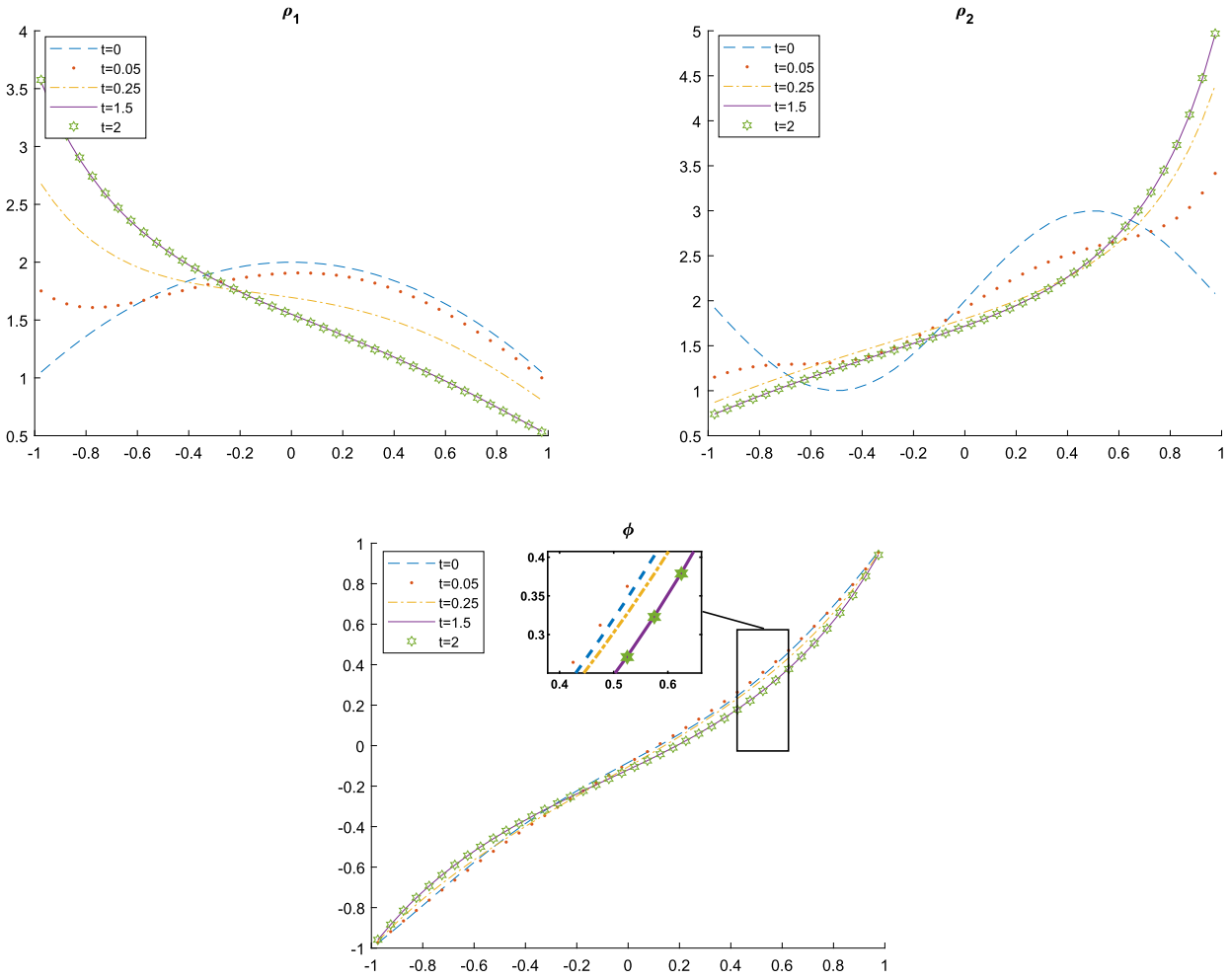

Fig. 1. Solution evolutions for ρ_1, ρ_2, and ϕ.

Example 5.2. In this test, still with the initial boundary value problem (5.1)-(5.2), we show the proven solution properties. We take $h = 0.05, \tau = 0.01$ to compute the numerical solutions up to $T = 2$. Solutions at $T = 0,\ 0.05,\ 0.25,\ 1.5,\ 2$ are given in Fig. 1. In Fig. 2 are total mass of ρ_1 and ρ_2 (the right vertical axis), and free energy profile (the left vertical axis). We see from Fig. 1 and Fig. 2 that the scheme is positivity preserving, mass conservative, and energy dissipating.

Example 5.3 *(Positivity propagation).* In this test, we consider the PNP system (5.1) with following initial and boundary conditions

$$\begin{aligned} &\rho_1^{in}(x) = \frac{10}{3}\chi_{[-0.5,0.5]}, \quad \rho_2^{in}(x) = 2 + sin(\pi x), \\ &\phi(0,t) = -1,\ \phi(1,t) = 1. \end{aligned} \tag{5.3}$$

We take $h = 0.05, \tau = 0.01$ to compute the numerical solutions up to $T = 2$. Solutions at $T = 0,\ 0.015,\ 0.1,\ 1,\ 2$ are displayed in Fig. 3. In Fig. 4 are total mass of ρ_1, ρ_2, and free energy profile. From these results we see that the scheme

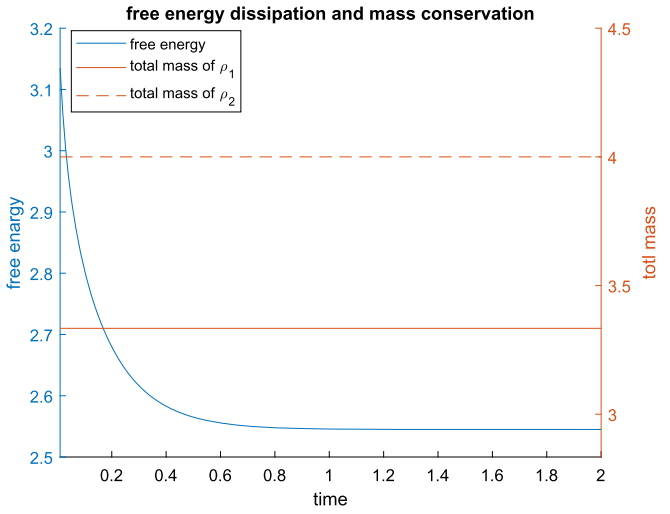

Fig. 2. Energy dissipation and mass conservation. (For interpretation of the colors in the figure(s), the reader is referred to the web version of this article.)

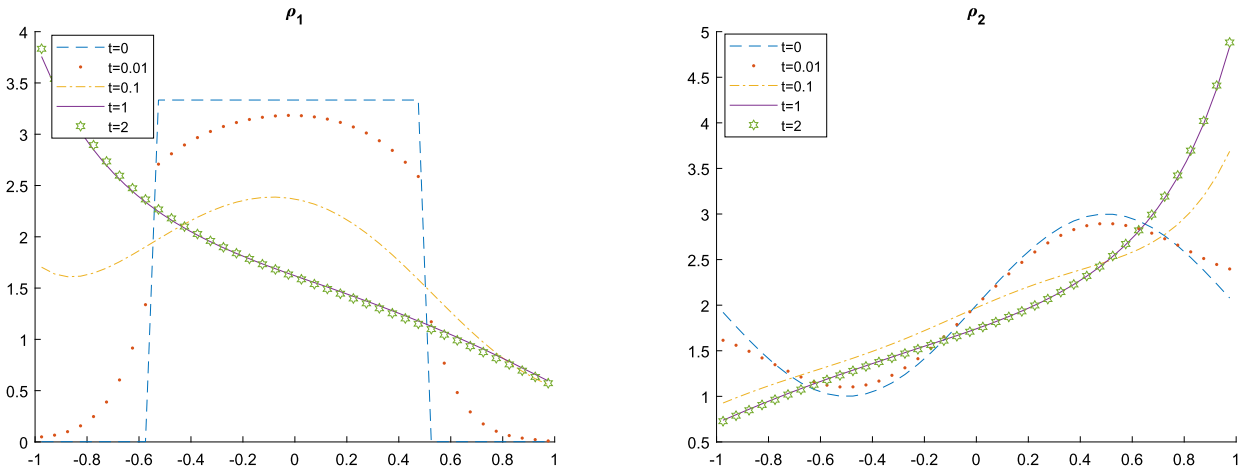

Fig. 3. Solution evolutions for ρ_1, ρ_2.

is positivity preserving, mass conservative, and energy dissipating. We also observe that steady state solutions are identical to those in Example 5.2; this suggests that steady state solutions of the PNP systems with the Dirichlet boundary condition only depends on the total mass and the boundary condition, but not sensitive to the profile of the initial data.

We attempted at applying the PDIP method to solve the minimization problem (4.1) and found it slow. To be more precise, let us compare PG with PDIP in terms of the computational cost. Motivated by perturbed KKT conditions the PDIP algorithm updates both primal and dual variables by taking one Newton step per iteration. PDIP methods are typically quite efficient. Under suitable conditions they have better than linear convergence. However, for numerical tests presented in this work, we found it much more expensive than the PG method. The PG method only requires inversion of $AA^\top$ once, hence more efficient. In Table 3 we compare CPU times (in seconds) needed for solving system (5.1) with initial and boundary conditions (5.3) when using the PDIP method and the PG method. Here we set $T = 0.5$ and choose different number of sub-intervals.

5.2. 2D single and multiple species

We further apply our scheme to solve the 2D PNP system and verify the proven properties.

Example 5.4. 2D single species (Neumann boundary condition). We now apply our scheme to solve the 2D single-species PNP system

$$\partial_t \rho = \nabla \cdot (\nabla \rho + \rho \nabla \phi),$$

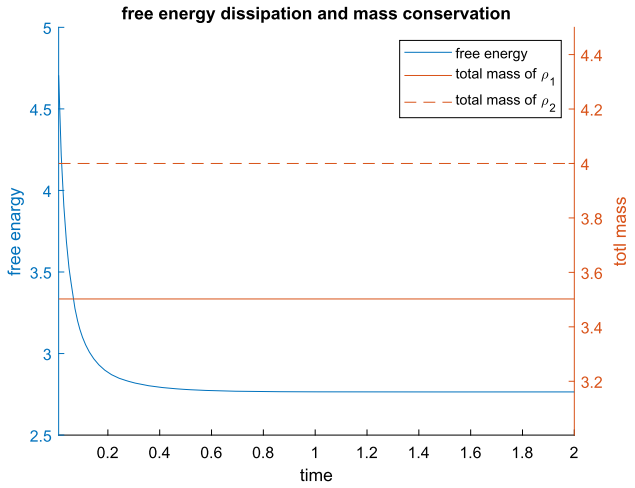

Fig. 4. Energy dissipation and mass conservation.

Table 3
CPU times comparison for PDIP method and PG method.

h	1/10	1/50	1/100	1/150	1/200	1/20	1/300
PDIP	1.22	2.37	8.38	17.73	31.32	48.97	74.71
PG	0.19	0.39	1.15	2.02	3.12	4.56	6.38

$$-\Delta\phi = \rho + f(x, y),$$

on domain $\Omega = [0, 1] \times [0, 1]$. We consider the initial boundary conditions

$$\rho^{in}(x, y) = -4(x^2 - x) - 8(y^2 - y), \quad \frac{\partial\phi}{\partial n}|_{\partial\Omega} = -1.$$

The permanent charge $f(x, y)$ is

$$f(x, y) = \begin{cases} 32, & \frac{5}{8} \le x \le \frac{7}{8}, \quad \frac{5}{8} \le y \le \frac{7}{8}, \\ 0, & else. \end{cases} \tag{5.4}$$

This problem satisfies the compatibility condition (2.4). We take $h_x = h_y = 0.025, \tau = 0.01$ to compute the numerical solutions up to $T = 6$. Color plot of the solutions at $T = 0.01, 0.5, 1, 2, 4, 6$ are given in Fig. 5. In Fig. 6 are total mass of ρ and free energy profile.

Example 5.5. 2D multiple species (Mixed boundary conditions). In this test, we solve the 2D multi-species PNP system

$$\begin{aligned} \partial_t \rho_1 &= \nabla \cdot (\nabla\rho_1 + \rho_1 \nabla\phi), \\ \partial_t \rho_2 &= \nabla \cdot (\nabla\rho_2 - \rho_2 \nabla\phi), \\ -\Delta\phi &= \rho_1 - \rho_2 + f(x, y), \end{aligned}$$

on domain $\Omega = [0, 1] \times [0, 1]$. We consider the initial boundary conditions

$$\begin{aligned} &\rho_1^{in}(x, y) = 4x(1 - x) + 8y(1 - y), \\ &\rho_2^{in}(x, y) = \sin(\pi x) + \sin(\pi y), \\ &\phi = 0 \text{ on } \partial\Omega_D, \text{ and } \frac{\partial\phi}{\partial n}|_{\partial\Omega} = -1 \text{ on } \partial\Omega_N, \end{aligned}$$

where $\partial\Omega_D = \{(x, y) \in \Omega : x = 0, x = 1\}$ and $\partial\Omega_N = \partial\Omega \setminus \partial\Omega_D$. The permanent charge $f(x, y)$ is

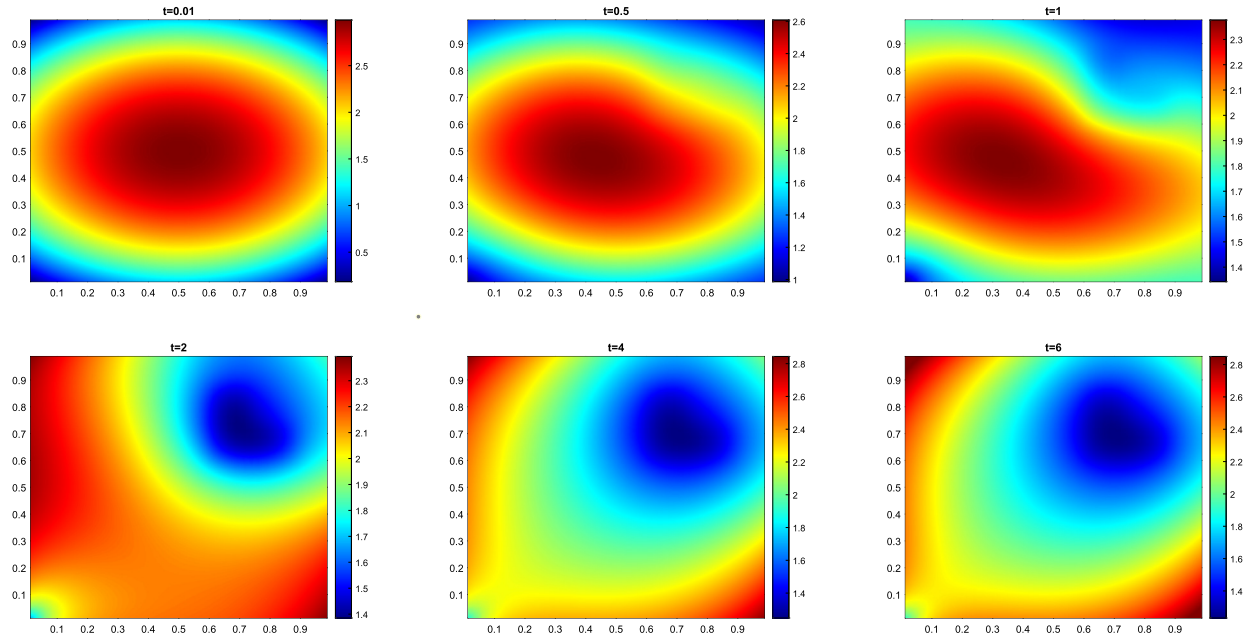

Fig. 5. Solution evolutions for ρ.

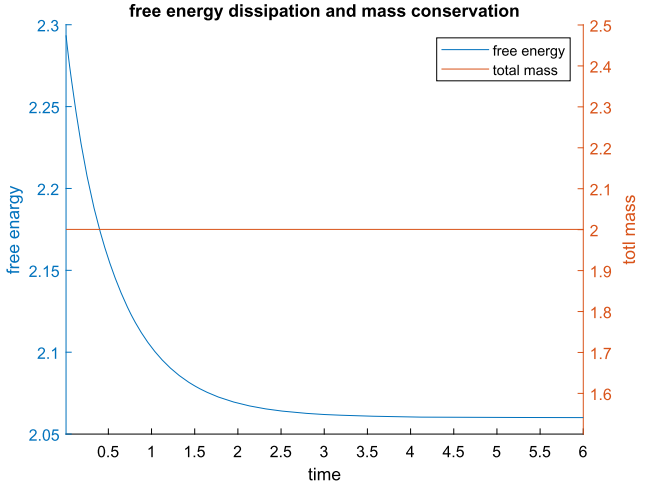

Fig. 6. Energy dissipation and mass conservation.

$$f(x,y)=\begin{cases}8, & \frac{5}{8}\le x\le\frac{7}{8},\quad \frac{5}{8}\le y\le\frac{7}{8},\\ 0, & else.\end{cases}$$

We take $h_x = h_y = 0.025, \tau = 0.001$ to compute the numerical solutions up to $T = 1$. Color plot of the solutions ρ_1 (first row) and ρ_2 (second row) at $T = 0.1, 0.2, 0.3, 0.5$ are given in Fig. 7, showing the density evolution profiles obtained by our proposed numerical scheme. From Fig. 7 we see that the positively charged ρ_1 diffused away from the center of the domain and the lowest concentration accrued near top right corner (this is where we placed the permanent charge f). The negatively charged ρ_2 moved towards the region where we placed the permanent charge.

In addition, we demonstrate the performance of our numerical scheme in preserving physical properties at a discrete level. With zero-flux boundary conditions, the total mass of concentrations over the computational domain should be conserved for each time step. This is perfectly confirmed in Fig. 8(a) for both ρ_1 and ρ_2. Displayed in this figure is also the discrete free energy profile, one can observe that it decreases monotonically (energy dissipating), as predicted in our numerical analysis. The free energy profile also suggests that the solutions approach the steady state at around $t = 0.5$. To verify the positivity-preserving property, we focus on the evolution of the minimum concentration for ρ_1 and ρ_2 over time interval

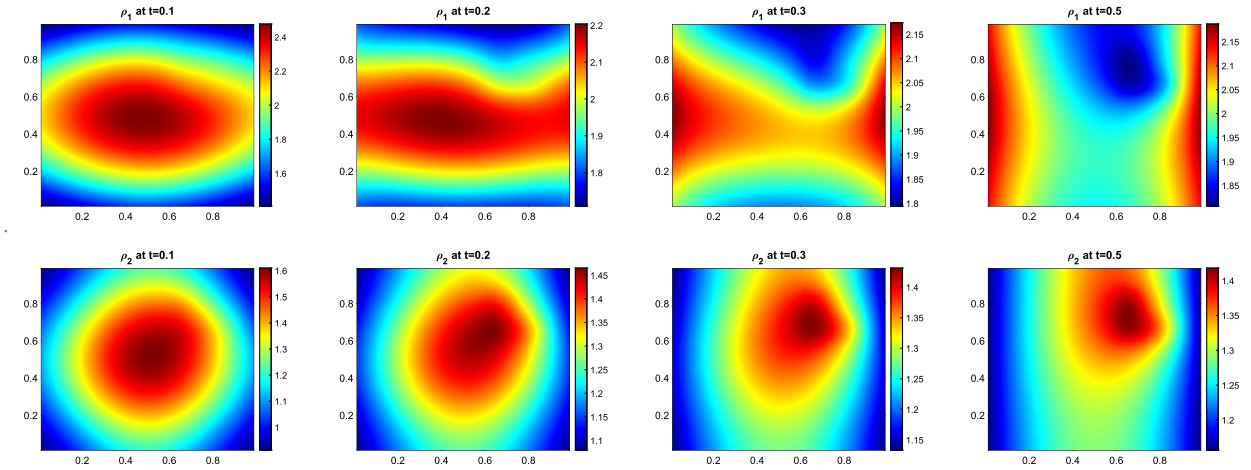

Fig. 7. Solution evolutions for ρ_1 and ρ_2.

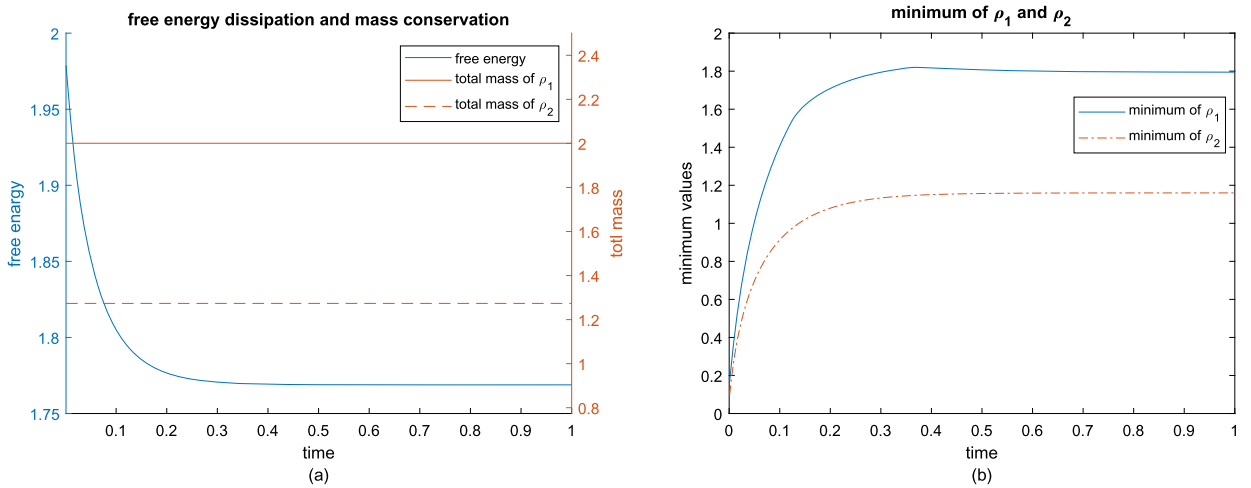

Fig. 8. Energy dissipation, mass conservation, and positivity.

$(0, 1]$. As shown in Fig. 8(b) the numerical density functions remain positive all the time, even though the concentrations are initially low near domain boundary.

6. Concluding remarks

In this paper, a dynamic mass transport method for the PNP system is established by drawing ideas from both the JKO-type scheme [23,26] and the classical Bennamou-Breiner formulation [3]. The energy estimate resembles the physical energy law that governs the PNP system in the continuous case, where the JKO type formulation is an essential component for preserving intrinsic solution properties. Both mass conservation and the energy stability are shown to hold, irrespective of the size of time steps. To reduce computational cost, we use a local approximation for the artificial time in the constraint transport equation by a one step difference and the integral in time by a one term quadrature.

Furthermore, by imposing a centered finite difference discretization in spatial variables, we establish the solvability of the constrained optimization problem. This also leads to a remarkable result: for any fixed time step and spatial meth size, density positivity will be propagating over all time steps, which is desired for any discrete version of the PNP system.

In the previous section, some numerical experiments were carried out to demonstrate the proven properties of a computed solution. The first experiment numerically verified that the variational scheme yields convergence to the solution of the nonlinear PDE with desired accuracy. Secondly, with further numerical tests the computed solutions are also shown to satisfy the energy dissipation law for the PNP system, mass conservation, and positivity propagation. It is a matter of future work to prove an error estimate for these numerical solutions. This is not a standard error analysis due to the nonlinearities in these problems, as well as the reformulation as a constrained optimization problem. This method is expected

to be extended to more complex PNP models such as PNP equations for semiconductor devices and three-dimensional ion channels.

CRediT authorship contribution statement

Authors have equal contribution.

Declaration of competing interest

The authors declare that they have no known competing financial interests or personal relationships that could have appeared to influence the work reported in this paper.

Data availability

Data will be made available on request.

Acknowledgements

This research was partially supported by the National Science Foundation under Grant DMS1812666.

References

[1] L. Ambrosio, N. Gigli, G. Savaré, Gradient Flows in Metric Spaces and in the Space of Probability Measures, Lect. Math., ETH Zürich, Birkhäuser Verlag, Basel, 2005.
[2] M.Z. Bazant, K. Thornton, A. Ajdari, Diffuse-charge dynamics in electrochemical systems, Phys. Rev. E 70 (2004) 021506.
[3] J.D. Benamou, Y. Brenier, A computational fluid mechanics solution to the Monge-Kantorovich mass transfer problem, Numer. Math. 84 (2000) 375–393.
[4] J.D. Benamou, G. Carlier, M. SLaborde, An augmented Lagrangian approach to Wasserstein gradient flows and applications, in: Gradient Flows: from Theory to Application, in: ESAIM Proc. Surveys., vol. 54, 2016, pp. 1–17.
[5] M. Burger, B. Schlake, M.-T. Wolfram, Nonlinear Poisson-Nernst-Planck equations for ion flux through confined geometries, Nonlinearity 25 (2012) 961–990.
[6] C. Cancès, T.O. Gallouët, G. Todeschi, A variational finite volume scheme for Wasserstein gradient flows, arXiv preprint arXiv:1907.08305, 2019.
[7] J.A. Carrillo, K. Craig, F.S. Patacchini, A blob method for diffusion, in: The Back-and-Forth Method for Wasserstein Gradient Flows, Calc. Var. Partial Differ. Equ. 58 (2) (2019) 53.
[8] J.A. Carrillo, B. Düring, D. Matthes, M.S. McCormick, A Lagrangian scheme for the solution of nonlinear diffusion equations using moving simplex meshes, J. Sci. Comput. 73 (3) (2018) 1463–1499.
[9] J.A. Carrillo, K. Craig, L. Wang, C. Wei, Primal dual methods for Wasserstein gradient flows, Found. Comput. Math. 22 (2022) 389–443.
[10] D. Chen, R. Eisenberg, Poisson-Nernst-Planck (PNP) theory of open ionic channels, Biophys. J. 64: A22 (1993).
[11] J. Ding, Z. Wang, S. Zhou, Positivity preserving finite difference methods for Poisson-Nernst-Planck equations with steric interactions: application to slit-shaped nanopore conductance, J. Comput. Phys. 397 (2019) 108864.
[12] J. Ding, C. Wang, S. Zhou, Convergence analysis of structure-preserving numerical methods based on Slotboom transformation for the Poisson–Nernst–Planck equations, arXiv:2202.10931, 2022.
[13] B. Eisenberg, Ionic channels in biological membranes - electrostatic analysis of a natural nanotube, Contemp. Phys. 39 (6) (1998) 447–466.
[14] A. Flavell, M. Machen, R. Eisenberg, J. Kabre, C. Liu, X. Li, A conservative finite difference scheme for Poisson-Nernst-Planck equations, J. Comput. Electron. 15 (2013) 1–15.
[15] A. Flavell, J. Kabre, X. Li, An energy-preserving discretization for the Poisson-Nernst-Planck equations, J. Comput. Electron. 16 (2017) 431–441.
[16] H. Gao, D. He, Linearized conservative finite element methods for the Nernst-Planck-Poisson equations, J. Sci. Comput. 72 (2017) 1269–1289.
[17] D. He, K. Pan, An energy preserving finite difference scheme for the Poisson-Nernst-Planck system, Appl. Math. Comput. 287 (2016) 214–223.
[18] D. He, K. Pan, X. Yue, A positivity preserving and free energy dissipative difference scheme for the Poisson-Nernst-Planck system, J. Sci. Comput. 81 (2019) 436–458.
[19] J.W. Hu, X.D. Huang, A fully discrete positivity-preserving and energy-dissipative finite difference scheme for Poisson-Nernst-Planck equations, Numer. Math. 145 (2020) 77–115.
[20] X. Huo, H. Liu, A.E. Tzavaras, S. Wang, An energy stable and positivity-preserving scheme for the Maxwell-Stefan diffusion system, SIAM J. Numer. Anal. 59 (5) (2021) 2321–2345.
[21] J.W. Jerome, Consistency of semiconductor modeling: an existence/stability analysis for the stationary Van Roosbroeck system, SIAM J. Appl. Math. 45 (4) (1985) 565–590.
[22] S. Ji, W. Liu, Poisson-Nernst-Planck systems for ion flow with density functional theory for hard-sphere potential: I-V relations and critical potentials. Part I: analysis, J. Dyn. Differ. Equ. 24 (2012) 955–983.
[23] R. Jordan, D. Kinderlehrer, F. Otto, The variational formulation of the Fokker- Plank equation, SIAM J. Math. Anal. 29 (1) (1998) 1–17.
[24] O. Junge, D. Matthes, H. Osberger, A fully discrete variational scheme for solving nonlinear Fokker–Planck equations in multiple space dimensions, J. Numer. Anal. 55 (1) (2017) 419–443.
[25] D. Kinderlehrer, N.J. Walkington, Approximation of parabolic equations using the Wasserstein metric, ESAIM: M2AN 33 (4) (1999) 837–852.
[26] D. Kinderlehrer, L. Monsaingeon, X. Xu, A Wasserstein gradient flow approach to Poisson-Nernst-Planck equations, ESAIM Control Optim. Calc. Var. 23 (1) (2017) 137–164.
[27] J.M. Lee, W. Jun, L. Flavien, The back-and-forth method for Wasserstein gradient flows, ESAIM Control Optim. Calc. Var. 27 (2021) 28.
[28] W.C. Li, J.F. Lu, L. Wang, Fisher information regularization schemes for Wasserstein gradient flows, J. Comput. Phys. 416 (2020) 109449.
[29] H. Liu, W. Maimaitiyiming, Energy stable and unconditional positive schemes for a reduced Poisson-Nernst-Plank system, Commun. Comput. Phys. 7 (5) (2020) 1505–1529.
[30] H. Liu, W. Maimaitiyiming, Efficient, positive, and energy stable schemes for multi-D Poisson–Nernst–Planck systems, J. Sci. Comput. 87 (3) (2021) 1–36.
[31] H. Liu, Z. Wang, A free energy satisfying finite difference method for Poisson-Nernst-Planck equations, J. Comput. Phys. 268 (2014) 363–376.

[32] H. Liu, Z. Wang, A free energy satisfying discontinues Galerkin method for one-dimensional Poisson-Nernst-Planck systems, J. Comput. Phys. 328 (2017) 413–437.
[33] H. Liu, Z. Wang, P. Yin, H. Yu, Positivity-preserving third order DG schemes for Poisson–Nernst–Planck equations, J. Comput. Phys. 452 (2022) 110777.
[34] W. Liu, Geometric singular perturbation approach to steady state Poisson-Nernst-Planck systems, SIAM J. Appl. Math. 65 (3) (2005) 754–766.
[35] C. Liu, C. Wang, S.M. Wise, X. Yue, S. Zhou, A positivity-preserving, energy stable and convergent numerical scheme for the Poisson-Nernst-Planck system, Math. Comput. 90 (331) (2021) 2071–2106.
[36] P.A. Markowich, C.A. Ringhofer, C. Schmeiser, Semiconductor Equations, Springer-Verlag, 1990.
[37] D. Matthes, S. Plazotta, A variational formulation of the BDF2 method for metric gradient flows, ESAIM: M2AN 53 (2019) 145–172.
[38] D. Matthes, H. Osberger, Convergence of a variational Lagrangian scheme for a nonlinear drift diffusion equation, Math. Model. Numer. Anal. 48 (3) (2014) 697–726.
[39] M.S. Metti, J. Xu, C. Liu, Energetically stable discretizations for charge transport and electrokinetic models, J. Comput. Phys. 306 (2016) 1–18.
[40] J. Nocedal, S.J. Wright, Numerical Optimization, Springer, 2006.
[41] F. Otto, The back-and-forth method for Wasserstein gradient flows, in: The Geometry of Dissipative Evolution Equations: The Porous Medium Equation, Commun. Partial Differ. Equ. 26 (1–2) (2001) 101–174.
[42] G. Peyré, The back-and-forth method for Wasserstein gradient flows, SIAM J. Imaging Sci. 8 (4) (2015) 2323–2351.
[43] J.H. Park, J. Jerome, Qualitative properties of steady-state Poisson-Nernst-Planck systems: mathematical study, SIAM J. Appl. Math. 57 (3) (1997) 609–630.
[44] S. Selberherr, Analysis and Simulation of Semiconductor Devices, Springer-Verlag/Wien, New York, 1984.
[45] J. Shen, J. Xu, Unconditionally positivity preserving and energy dissipative schemes for Poisson-Nernst-Planck equations, Numer. Math. 148 (3) (2021) 671–697.
[46] R. Shen, Q. Zhang, B. Lu, An inverse averaging finite element method for solving the size-modified Poisson-Nernst-Planck equations in ion channel simulations, arXiv:2112.01692, 2021.
[47] T. Teorell, Transport processes and electrical phenomena in ionic membranes, Prog. Biophys. 3 (1953) 305.